LATERAL FORCES ON HYDRAULIC PISTONS

CAUSED BY AXIAL LEAKAGE FLOW

by

HELMUT ERNST WEBER

SUBMITTED IN PARTIAL FULFILLMENT OF THE
REQUIREMENTS FOR THE DEGREE OF
MASTER OF SCIENCE

at the

MASSACHUSETTS INSTITUTE OF TECHNOLOGY
(1951)

Signature Redacted

Signature of Author ....
Department of Mechanical Engineering
August 20, 1951

Signature Redacted

Certified by...
Thesis Supervisor

Signature Redacted

....
Chairman, Departmental Committee on Graduate Students

ABSTRACT

Hydraulic pistons are often used with low force level actuators to control high pressure fluid flow. The lateral forces arising from the leakage flow between the bore and piston lands may cause large friction forces which in turn lead to erratic control. This paper is written in an endeavor to analyze the lateral forces resulting from various shapes and configurations of the land and bore as well as to evaluate the assumptions made in the mathematical analysis commonly employed.

The assumption that is least valid is that of one-dimensional flow. It is assumed that for short axial land lengths and for the boundary conditions of the flow the peripheral flow or pressure gradients are negligible, and that the flow is axial (parallel to the axis of the bore and piston land). Paradoxically then, the peripheral pressure gradient arising in the analysis is integrated around the surface of the land to obtain the lateral force acting on the piston. However, we have shown that although the lateral force on the land can become very large, the peripheral pressure gradients are small compared to the axial pressure gradients. The experimental results substantiate the assumptions made, and any discrepancies are explained qualitatively by a complete consideration of the flow phenomenon.

Tapers, high spots, steps and dirt on the land or bore surface of ordinary dimensions can cause an axial force on one land which attains a value of fifteen pounds. A lateral force of that magnitude and in a direction tending to force the land against the bore wall can result in a friction force that is large when an axial stroking force of only a few pounds is available. It is expected that the results obtained can permit land designs that utilize the lateral forces to maintain the piston land centered in the bore. In the centered position fluid will completely separate the surfaces, replacing dry friction with complete viscous friction.

ACKNOWLEDGEMENTS

The author wishes to express his sincere gratitude to Professor John A. Hrones who made this thesis possible; to J. Lowen Shearer for the topic suggestion and his helpful advice and encouragement as the work progressed. The author also extends many thanks to Thomas Garber and Charles Pazaree for the use of their Linearsyns; to Gerhard Reethof, Herbert Price, Thomas Kiely and the entire staff of the Dynamic Analysis and Control Laboratory for their constant cooperation.

TABLE OF CONTENTS

TABLE OF FIGURES

LIST OF SYMBOLS

a   Lateral displacement from axial centerline of bore.

C, C_1, C_2 Axial length of land

D   Diameter of land.

e   Amount of radial step.

F   Lateral force on one land.

F'   Lateral force per unit peripheral width.

F_n Dimensionless lateral force, $F/2r_o p_g C$.

f   Function.

g   Subscript referring to pressure drop from supply to exhaust pressure.

h, h_1, h_2 Clearances between flow surfaces.

I   Integral.

i $\sqrt{-1}$

k   A constant.

l   A characteristic average length dimension of the flow region.

p, p_s, p_a, p_g Pressure.

Q   Total flow rate.

Q'   Flow rate per unit width.

r, r_o, r_s Radial lengths of flow region and land.

t   Radial clearance between land and bore at centered position.

u   Velocity component in x-direction.

V   Characteristic average velocity in flow region.

v   Velocity component in y-direction.

w   Velocity component in z-direction.

x   Rectangular coordinate.

y   Rectangular coordinate.

z   Rectangular coordinate.

Greek

α Angle of a complex number.

γ Rotation of axial centerline of land
or angle of cocking.

μ Viscosity.

σ Angle of a complex number.

τ Dimensionless lateral displacement, a/t.

ω Cylindrical coordinate.

$_o$ refers to centered condition of land
and bore.

INTRODUCTION

Friction is ever present in all physical systems whether in static equilibrium or dynamic motion. Although in many applications its action is necessary, in an equally important number of applications its action is undesirable. The undesirable nature of friction is characterized by retarding force, unpredictable action, and wear.

To eliminate or as far as possible to alleviate these undesirable features of friction, use is made of the fact that fluid friction is much more desirable than dry or solid friction with respect to all three characteristics above. The entire science of lubrication arises from an attempt to replace dry friction by fluid friction. Fluid friction has several important advantages. Retarding force offered by fluid friction is much less than that offered by dry friction. Although the action of dry friction may be statistically predicted in time, the action of fluid friction is a far more simple function of the important variables. Further, if the viscosity of the fluid can be considered constant, fluid friction lends itself well to analytical investigation. Dry friction is a strong function of pressure normal to its direction of action, whereas fluid friction is not. Therefore, it would in many cases be desirable to replace dry friction by fluid friction under the same pressure.

In general to eliminate dry friction between two solid surfaces it must be possible to maintain fluid between

them at sufficient pressure to counteract any force tending to push them together. In this paper we will consider the fluid pressure distribution and resulting normal force on two surfaces whose separation is very small compared to the length and width of the surfaces. This type of fluid flow we shall designate as capillary flow.

CHAPTER I

PRELIMINARY ANALYSIS

In this paper we will consider lateral fluid force on a piston such as is employed in flow control. One or more pistons, operated with a low energy level supply, usually control high energy fluid flow, distributing it where and when necessary. Often the pistons are operated by a feed back signal from the controlled quantity, and when a condition of dry friction exists between piston land and cylinder wall, erratic and oscillatory operation often results.

In an attempt to replace dry friction by fluid friction we will analyze and measure experimentally the lateral force exerted by the fluid pressure on the piston land. As a first step we must analyze the pressure distribution in the flow region between the land and cylinder or bore wall for various piston land shapes and configurations of the piston and cylinder.

In many flow valves, where leakage must be held to a minimum, clearances between the piston lands and cylinder wall are of the order of a few ten-thousandths of an inch. Measurement of any lateral force with ordinary techniques and equipment is virtually impossible for such small clearances. Two further obstacles to accurate measurement are: the inaccuracies in grinding which are of the same order of magnitude as the clearances, and the presence of small dirt particles in the hydraulic oil which accumulate between the piston lands

and cylinder wall (a phenomenon referred to as silting).
Although the oil may be well filtered and the particles of
only a few microns in size, silting is observed when leakage
clearances are of the order of a few ten-thousandths of an
inch.

These considerations lead us to the use of a large
scale model, maintaining dynamic similarity.[1] In this way
we can relate the physical properties of the model to those
of the prototype.

From physical reasoning we can say that the lateral
force depends upon the pressure drop, a characteristic length,
the lateral displacement of the piston, and the viscosity of
the fluid. If we assume that capillary flow obtains, i.e.,
the surface area of flow is large compared to the volume,
inertia effects can be neglected. The lateral force is, there-
fore, not a function of the fluid density. Further, since there
are no free surfaces in the region of flow under consideration,
the lateral force is independent of gravity. Alternatively,
since the flow rate is a function of the pressure drop, we can
say that the lateral force depends upon the flow rate, a char-
acteristic length, the lateral displacement of the piston, and
the viscosity of the fluid. The two alternative equations are:

$$F = f_1(a, D, p, \mu)$$

$$F = f_2(a, D, Q, \mu)$$

1. J. C. Hunsaker and B. G. Rightmire, Engineering Applications of Fluid Mechanics, New York, McGraw-Hill, 1947, pp.113-116.

By dimensional analysis[2] we form the dimensionless quantities as follows:

$$\frac{F}{pD^2} = f_3 \left(\frac{a}{D}, D, p, \mu\right)$$

$$\frac{FD}{\mu Q} = f_4 \left(\frac{a}{D}, D, Q, \mu\right)$$

The remaining three dimensional variables cannot be combined to give another dimensionless quantity. Therefore, since a dimensionless quantity cannot be a function of dimensional quantities, we find

$$\frac{F}{pD^2} = f_5 \left(\frac{a}{D}\right)$$

$$\frac{FD}{\mu Q} = f_6 \left(\frac{a}{D}\right)$$

(1)

To maintain dynamic similarity, i.e., to relate data from the model to the prototype the dimensionless variables in Equation (1) must be maintained the same for the model as for the prototype. This is so because we know only the variables and their number and not the function.

A large scale model will greatly reduce the limitations imposed by machining inaccuracies and completely remove the effect of silting. The lateral force caused by leakage flow between the piston lands and cylinder can then be measured

----

2. Ibid, pp. 98-121.

for different land shapes and configurations as a function of piston displacement from the axial centerline of the cylinder.

If the model is made to a 10:1 scale and the same oil is used, then for dynamic similarity,

$$\left(\frac{F}{pD^2}\right)_m = \left(\frac{F}{pD^2}\right)_{pr}$$

$$\left(\frac{FD}{\mu Q}\right)_m = \left(\frac{FD}{\mu Q}\right)_{pr}$$

$$a_m = 10a_{pr}$$

$$D_m = 10\ D_{pr}$$

$$\mu_m = \mu_{pr}$$

$$P_m = \frac{1}{100}\ P_{pr}$$

$$Q_m = 10\ Q_{pr}$$

$$F_m = F_{pr}$$

The two quantities we are primarily interested in are lateral force and displacement or specifically we can investigate the relationship between them. With the aid of dimensional analysis as presented here we can experimentally determine the functional relationship given in Equation (1). First we will attempt to derive some helpful analytical facts about the flow region and resulting lateral force.

CHAPTER II

GENERAL CAPILLARY FLOW EQUATIONS

The general equations of fluid flow which take into consideration fluid inertia, viscous, and body forces are extremely complex, and exact mathematical solutions are at present impossible to obtain for any but the simplest cases. To permit analytical treatment these equations must be simplified.

In the flow of a viscous fluid between two neighboring surfaces where the volume of the flow region is small compared to the surface area inertia effects can be neglected. The only body force acting is gravity which is neglected because there are essentially no changes in elevation and no free surfaces in the flow region. Further it is assumed that in the thin flow region the flow is parallel to the surfaces, implying that there are no pressure gradients in the direction perpendicular to the bounding surfaces.

By the above assumptions the general flow equation of Navier-Stokes[3] reduces to:

$$\frac{\partial p}{\partial x} = \mu \left(\frac{\partial^2 u}{\partial x^2} + \frac{\partial^2 u}{\partial y^2} + \frac{\partial^2 u}{\partial z^2} \right) \tag{2}$$

_ _ _ _ _ _ _ _ _ _ _ _ _ _ _ _ _

3. L. Prandtl and O. G. Tietjens, _Fundamentals of Hydro and Aeromechanics_, New York, McGraw-Hill, 1934, p.258.

$$\frac{\partial p}{\partial y} = \mu(\frac{\partial^2 v}{\partial x^2} + \frac{\partial^2 v}{\partial y^2} + \frac{\partial^2 v}{\partial z^2})$$

$$\frac{\partial p}{\partial z} = 0$$

(2)

where the z coordinate is perpendicular to the surfaces (Figure 1). This equation can be simplified to obtain practical results without great effort. First we can make Equation (2) dimensionless.

Let $p' = \frac{p}{p_s}$; $u' = \frac{u}{V}$; $v' = \frac{v}{V}$; $x' = \frac{x}{l}$; $y' = \frac{y}{l}$; $z' = \frac{z}{l}$

where V is some average of the u and v velocity components and l is some average of the x and y dimensions of the flow region.

And Equations (2) can be written:

$$p_s \frac{\partial p'}{\partial x'} = \mu V(\frac{\partial^2 u'}{\partial x'^2} + \frac{\partial^2 u'}{\partial y'^2} + \frac{\partial^2 u'}{\partial z'^2})$$

$$p_s \frac{\partial p'}{\partial y'} = \mu V(\frac{\partial^2 v'}{\partial x'^2} + \frac{\partial^2 v'}{\partial y'^2} + \frac{\partial^2 v'}{\partial z'^2})$$

(3)

$$\frac{\partial p'}{\partial z'} = 0$$

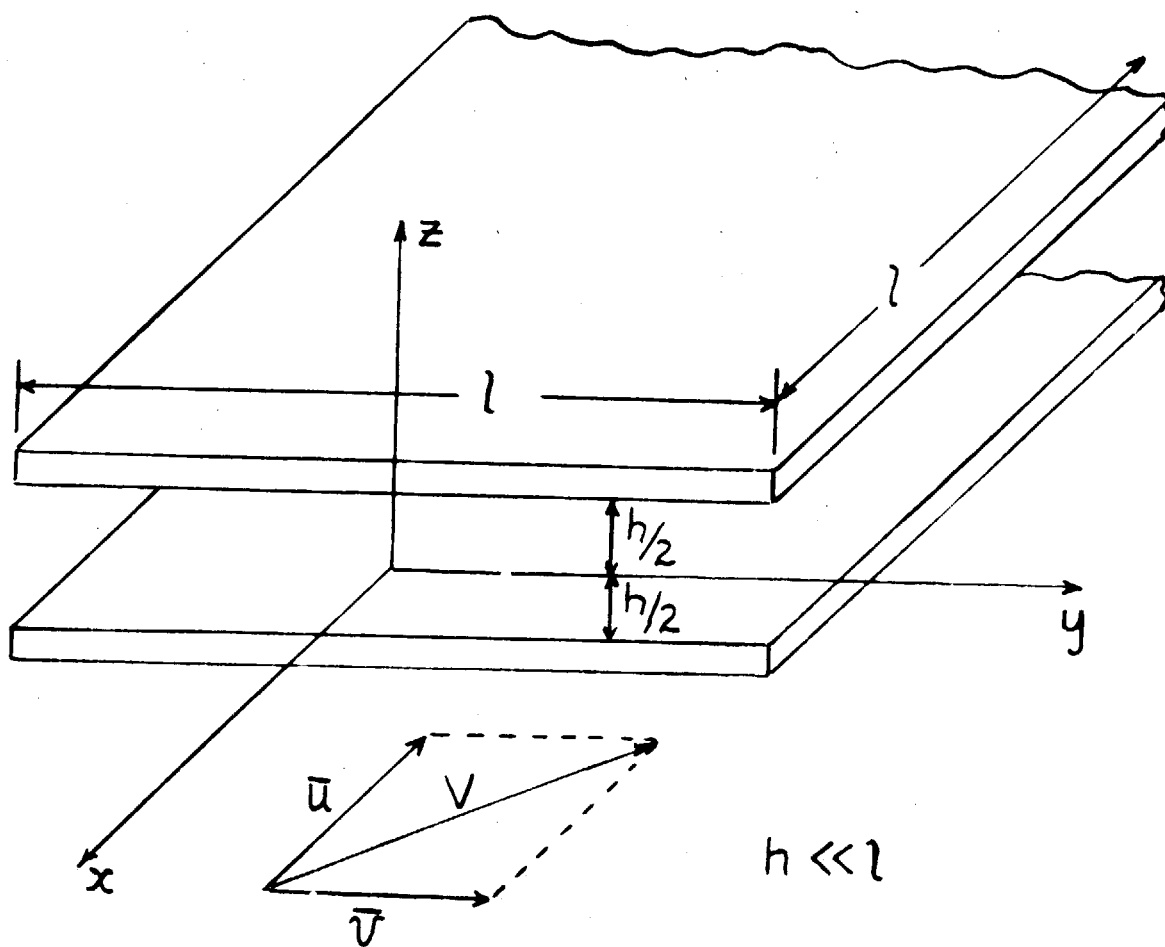We can next investigate the orders of magnitude of the various terms in the dimensionless Equations (3).

F I G. 1

By a suitable choice of the non-dimensionalizing quantities, V and l, we can write the following variables and their orders of magnitude

$$x' = 0\ [1] \qquad\qquad u' = 0\ [1]$$

$$y' = 0\ [1] \qquad\qquad v' = 0\ [1]$$

$$z' = 0[h'] \qquad\qquad w' = 0$$

where $h' = \dfrac{h}{l} = 0\left[\dfrac{1}{1000}\right]$

From these we can determine the following variables and their orders of magnitude

$$\frac{\partial u'}{\partial x'},\ \frac{\partial^2 u'}{\partial x'^2},\ \frac{\partial u'}{\partial y'},\ \frac{\partial^2 u'}{\partial y'^2},\ \frac{\partial v'}{\partial x'},\ \frac{\partial^2 v'}{\partial x'^2},\ \frac{\partial v'}{\partial y'},\ \frac{\partial^2 v'}{\partial y'^2} = 0\ [1]$$

$$\frac{\partial v'}{\partial z'},\ \frac{\partial u'}{\partial z'} = 0\left[\frac{1}{h'}\right] = 0[1000],\quad \frac{\partial^2 u'}{\partial z'^2},\ \frac{\partial^2 v'}{\partial z'^2} = 0\left[\frac{1}{h'}\right] = 0[1000]$$

Consequently, in the right hand members of Equations (3), the velocity derivatives with respect to x' and y' are negligible in comparison to the z' derivatives.

Equations (2) can now be written in the form

$$\frac{\partial p}{\partial x} = \mu\ \frac{\partial^2 u}{\partial z^2}$$

$$\frac{\partial p}{\partial y} = \mu\ \frac{\partial^2 v}{\partial z^2}$$

(4)

Since the pressure is uniform in the z- direction, $\frac{\partial p}{\partial y}$ and $\frac{\partial p}{\partial x}$ are independent of z. Integration of Equations (*) twice with respect to z and the application of the boundary condition that the velocity is zero at both surfaces $(z = \pm\, h/2)$ gives

$$u = -\frac{1}{2\mu}\frac{\partial p}{\partial x}\left[\left(\frac{h}{2}\right)^2 - z^2\right]$$

$$v = -\frac{1}{2\mu}\frac{\partial p}{\partial y}\left[\left(\frac{h}{2}\right)^2 - z^2\right]$$

The average velocity can be found over the cross-section, and the product of it and the gap clearance, h, gives flow per unit width. Finally we arrive at the equations of capillary flow expressing flow per unit width as a function of the surface separation and the component of the pressure gradient in the flow direction.

$$Q'_x = -\frac{h^3}{12\mu}\frac{\partial p}{\partial x}$$

$$Q'_y = -\frac{h^3}{12\mu}\frac{\partial p}{\partial y} \tag{5}$$

or

$$Q' = -\frac{h^3}{12\mu}\,\text{grad } p$$

where Q' is in the direction of the gradient of p. Note that if the flow is one dimensional, Equation (5) can be integrated immediately for the pressure distribution. However, for two dimensional flow Equation (5) can be put into more convenient form.

If the fluid is incompressible, the flow rate into a unit volume must be the same as that out, or mathematically

$$\text{div } Q' = - \text{div}\left(\frac{h^3}{12\mu} \text{ grad } p\right) = 0 \tag{6}$$

The viscosity is assumed constant, and Equation (6) reduces to

$$\text{div}\left(h^3 \text{ grad } p\right) = 0 \tag{7}$$

Equation (7) is the basic differential equation of capillary viscous fluid flow, solutions of which give the pressure distribution in a two dimensional coordinate system. In the cases we shall consider the coordinates are cylindrical, z and ω.

In general the flow between a land and cylinder bore is two dimensional in the peripheral and axial directions. Figure (1) illustrates the general region of flow. The pressure distribution and its gradients will vary, of course, with the three dimensional space configuration of bore and piston land. All configurations for a given land and bore can be reduced to a combination of radial displacement and z- axis rotation of the land relative to the bore, but alterations of the peripheral and axial shape of the land and bore add to the possible configurations.

Many piston land shapes can be considered, but by a judicious choice of a few the important physical character-

istics of the fluid flow can be deduced for any configuration and shape of land and bore. For all these possible configurations and shapes certain conditions will always hold for the flow region. They are as follows:

1. The entire flow occurs between surfaces separated by a distance which is very small compared to the extent of the surfaces.

2. The boundaries of the flow region at fluid entry and exit are subjected to constant but different pressures. These boundaries lie in planes perpendicular to the axial centerline or z- axis.

3. The pressure distribution is periodic of period 2π in the peripheral direction.

4. The fluid is incompressible.

5. The pressure distribution satisfies Equation (7).

$$\text{div} \left(h^3 \text{ grad } p \right) = 0 \qquad (7)$$

We will consider three principal types of lands. First is the case of a cylindrical land (round or out-of round), generated by lines parallel to the axis of the piston land, displaced radially and rotated axially, Figures (1a and 2b). Second is the case of a cylindrical land with a radial step displaced radially and rotated axially, Figure (4). Third is the case of the first land type in the position of a pressurized fluid bearing, Figure (6). Superposition of cases one

and two give information regarding the case of high spots on the surface of the land. All analytical results are checked experimentally wherever possible. In general from these three basic cases we can interpret how the pressure varies for changes and rates of change in the separation of the flow surfaces.

CHAPTER III

TWO DIMENSIONAL PRESSURE DISTRIBUTION
AROUND A RIGHT CIRCULAR, CYLINDRICAL LAND

Generally to permit easy analytical treatment the flow across the surface of a piston land is assumed axial, and it is assumed that peripheral flow or pressure gradients are negligible, i.e. for all types of lands considered fluid flows parallel to the axial centerline of the bore from the high constant pressure at one end of the land to the low constant pressure at the other end. This assumption is based on the premise that the axial land length is of the same order of magnitude as the peripheral length, and becomes more valid as the axial land length decreases. Analytical results give much greater average axial pressure gradients than the average peripheral pressure gradients which arise from such an assumption. These gradients will be compared later for orders of magnitude.

We can analytically investigate the true two-dimensional pressure distribution for the case of a right circular, cylindrical land with a pure lateral displacement from the axial centerline. For this case the gap height between the flow surfaces is a function of the peripheral coordinate, ω, only and is constant in the axial direction, Figure (2). By physical symmetry when the lateral displace-

FIG. 2a

$h, t \ll r_o$
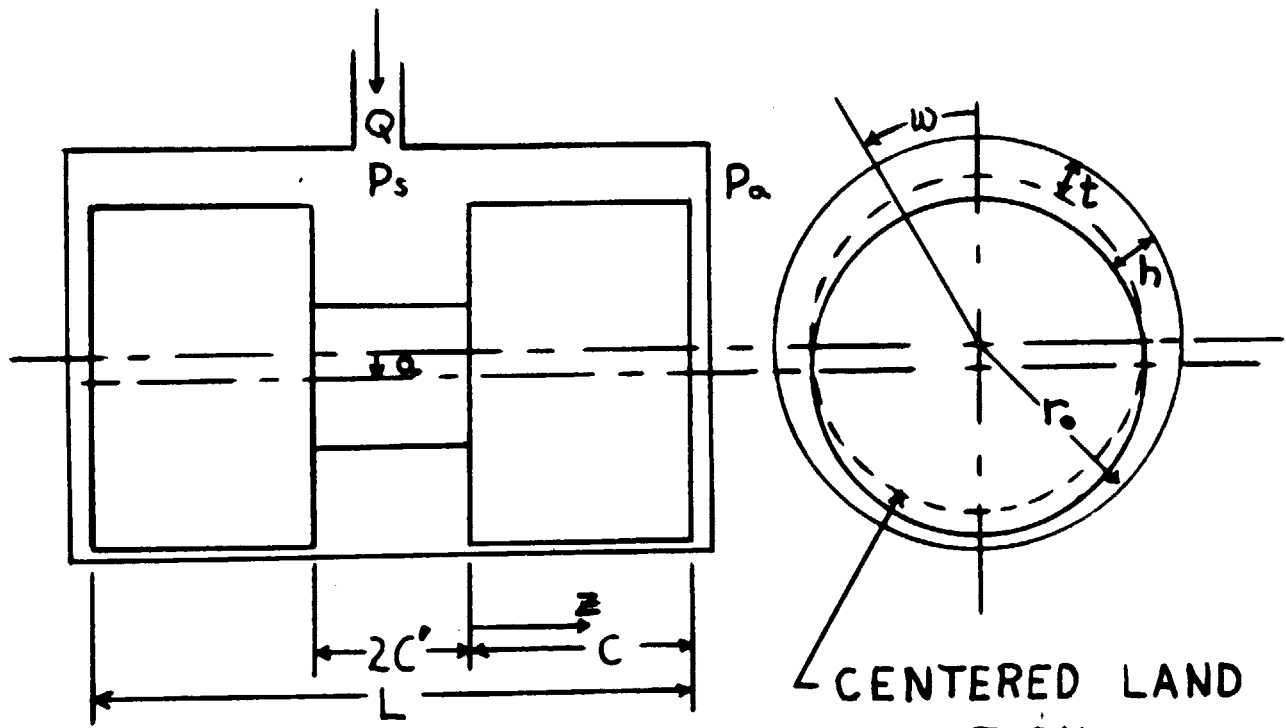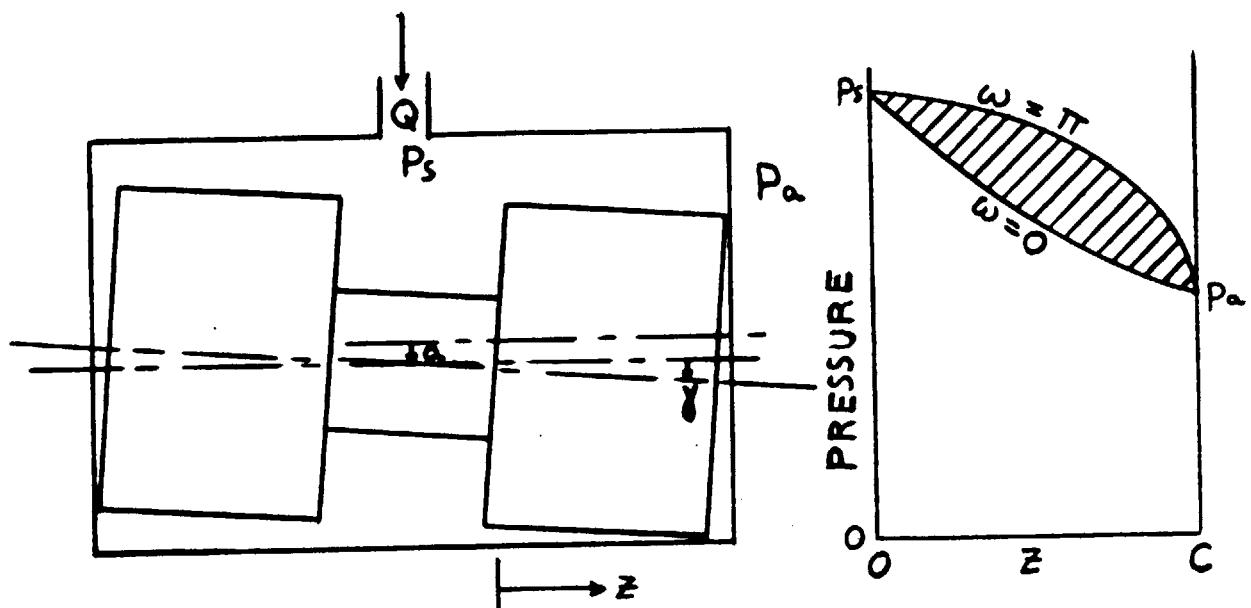

FIG. 2b

ment is zero (the piston is perfectly centered in the bore) the flow is purely axial since the gap height is the same everywhere and an axial pressure drop is imposed on the boundaries. When the piston is laterally displaced, the gap height changes around the periphery and physically we might imagine that this change in gap height will produce peripheral flow or pressure gradients. We can now proceed to show that this is not true, that the flow will remain purely axial, and that no lateral force on the piston land obtains.

Consideration of the geometry of the piston when displaced laterally downward gives for the gap height,

$$h = t + a \cos \omega$$

For convenience we can substitute the dimensionless displacement parameter

$$\tau = \frac{a}{t}$$

and express the gap height as

$$h = t(1 + \tau \cos \omega) \tag{8}$$

Substituting this expression for h in Equation (7) and expanding we obtain the basic differential equation which must be satisfied by the pressure as

$$(1 + \tau \cos \omega)^3 \frac{\partial^2 p}{\partial z^2} + \frac{1}{r_o^2} \frac{\partial}{\partial \omega}\left[(1 + \tau \cos \omega)^3 \frac{\partial p}{\partial \omega}\right] = 0 \tag{9}$$

The solution of this equation combined with the boundary conditions of the flow region results in the pressure distribution on the surface of the land, and the component of lateral force in any direction can be found by an integration of the pressure component over the area of the land.

Boundary conditions which must be satisfied by the pressure at each end of the land are

$$p(z,\omega)_{z=0} = p_s$$

$$p(z,\omega)_{z=C} = p_a$$

(10)

Two further boundary conditions can be derived by noting from physical symmetry that the pressure must be an even function of ω, i.e., $p(z,\omega) = p(z,-\omega)$, and must be periodic in ω of period 2π. This means that the rate of change of pressure in the direction of ω must be zero at both, $\omega = 0$ and π or

$$\left(\frac{\partial p}{\partial \omega}\right)_{\omega=0,\pi} = 0$$

(11)

The pressure gradient at those values of ω must be axial and consequently the flow must be axial at $\omega = 0$, π. Then because the fluid is incompressible the flow rate per unit peripheral width, Q', at those points of ω is constant for all z. Since h is a function of ω only, it is also constant with z. These considerations hold true regardless of

the lateral displacement and therefore the pressure gradient at $\omega = 0$, π is axial and constant. Rewriting Equations (5) in cylindrical coordinates yields

$$Q'_z = -\frac{h^3}{12\mu}\frac{\partial p}{\partial z} \tag{5a}$$

$$Q'_\omega = -\frac{h^3}{12\mu}\frac{\partial p}{r_0\,\partial\omega} \tag{5b}$$

$$Q' = -\frac{h}{12\mu}\,\text{grad } p \tag{5c}$$

Noting that $(\text{grad } p)_{\omega=0,\pi} = \left(\frac{\partial p}{\partial z}\right)_{\omega=0,\pi}$

$$(dp)_{\omega=0,\pi} = \frac{12\mu}{h^3}\,Q'\,dz \tag{12}$$

Integrating this equation and eliminating Q' by using the condition that at $z = 0$ and C, $p = p_g$ and p_a respectively, yields for the pressure

$$p_{\omega=0,\pi} = p_g\left(1-\frac{z}{C}\right) + p_a \tag{13}$$

Equations (10 and 13) give four boundary conditions that the solution to Equation (9) must satisfy.

We assume that the pressure can be expanded in a power series as follows

$$\tag{14}$$
$$p(z,\,\omega) = p_0(z,\,\omega) + \tau\,p_1(z,\,\omega) + \tau^2 p_2(z,\,\omega) + \cdots + \tau^n p_n(z,\,\omega)$$

From Equation (8) and the definition of τ note that $0 \leqslant \tau \leqslant 1$ ($\tau = 1$ when the land contacts the wall of the bore). If the p_n's are bounded, this series will converge for all τ less than one. Substitution of series (14) into Equation (9) and rearrangement of terms yields

$$\frac{\partial^2 p_0}{\partial z^2} + \frac{1}{r_0^2} \frac{\partial^2 p_0}{\partial \omega^2} + \tau \left[\frac{\partial^2 p_1}{\partial z^2} + \frac{1}{r_0^2} \frac{\partial^2 p_1}{\partial \omega^2} + \frac{\partial}{\partial z} (3 \cos \omega \frac{\partial p_0}{\partial z}) + \right.$$

$$\left. \frac{1}{r_0^2} \frac{\partial}{\partial \omega} (3 \cos \omega \frac{\partial p_0}{\partial \omega}) \right] + \tau^2 \left[\frac{\partial^2 p_2}{\partial z^2} + \frac{1}{r_0^2} \frac{\partial^2 p_2}{\partial \omega^2} + \right.$$

$$\frac{\partial}{\partial z} (3 \cos \omega \frac{\partial p_1}{\partial z} + 3 \cos^2 \omega \frac{\partial p_0}{\partial z}) + \frac{1}{r_0^2} \frac{\partial}{\partial \omega} (3 \cos \omega \frac{\partial p_1}{\partial \omega} +$$

$$\left. 3 \cos^2 \omega \frac{\partial p_0}{\partial \omega}) \right] + \cdots = 0 \tag{15}$$

The p_n's are independent of τ and if Equation (15) is to be valid for all values of τ, the coefficients of the τ^n's must be independently equal to zero.

$$\frac{\partial^2 p_0}{\partial z^2} + \frac{1}{r_0^2} \frac{\partial^2 p_0}{\partial \omega^2} = 0 \tag{16a}$$

$$\frac{\partial^2 p_1}{\partial z^2} + \frac{1}{r_0^2} \frac{\partial^2 p_1}{\partial \omega^2} + \frac{\partial}{\partial z} (3 \cos \omega \frac{\partial p_0}{\partial z}) + \frac{1}{r_0^2} \frac{\partial}{\partial \omega} (3 \cos \omega \frac{\partial p_0}{\partial \omega}) = 0 \tag{16b}$$

$$\frac{\partial^2 p_2}{\partial z^2} + \frac{1}{r_o^2} \frac{\partial^2 p_2}{\partial \omega^2} + \frac{\partial}{\partial z}(3 \cos \omega \frac{\partial p_1}{\partial z} + 3 \cos^2 \omega \frac{\partial p_o}{\partial z}) +$$

$$\frac{1}{r_o^2} \frac{\partial}{\partial \omega}(3 \cos \omega \frac{\partial p_1}{\partial \omega} + 3 \cos^2 \omega \frac{\partial p_o}{\partial \omega}) = 0 \qquad (16c)$$

Similarly for every coefficient of τ^n.

Series (14) shows that p_o represents the pressure when τ is zero or when the piston is centered in the bore. For this position the gap height is everywhere constant and complete radial symmetry obtains. This implies that the flow must be purely axial for $\tau = 0$. Equation (5c) again gives the gradient of p as axial and constant or the pressure is

$$p_{\tau=0} = p_o = p_g(1 - \frac{z}{C}) + p_a \qquad (17)$$

which is the solution for Equation (16a).

We must now find the solution p_1 for Equation (16b). Substituting p_o from Equation (17) into (16b) yields

$$\frac{\partial^2 p_1}{\partial z^2} + \frac{1}{r_o^2} \frac{\partial^2 p_1}{\partial \omega^2} = 0 \qquad (18)$$

Before proceeding to a solution we will determine the boundary conditions that must be satisfied by p_1. Writing that the pressure at $z = 0$ is p_s obtains from Series (14)

$$p(0,\omega) = p_s = p_o(0,\omega) + \tau p_1(0,\omega) + \tau^2 p_2(0,\omega) + \cdots$$

Substituting p_0 from Equation (17) and subtracting p_s from each side of the equation yields

$$0 = \tau\, p_1(0,\omega) + \tau^2 p_2(0,\omega) + \cdots \cdot \tag{19}$$

If this equation is to be true for all τ, all the $p_n(0,\omega)$'s must be each equal to zero. A similar application of the boundary condition stating that the pressure at $z = C$ is p_a yields another exactly similar boundary condition. Two boundary conditions for p_1 then result as

$$p_1(0,\omega) = 0$$
$$p_1(C,\omega) = 0 \tag{20}$$

Application of the boundary condition Equation (13) in the same way to Series (14) yields

$$p_1(z,0) = 0$$
$$p_1(z,\pi) = 0 \tag{21}$$

and in general it is found that

$$p_n(0,\omega) = 0$$
$$p_n(C,\omega) = 0$$
$$p_n(z,0) = 0$$
$$p_n(z,\pi) = 0 \tag{22}$$

Equation (18) which p_1 must satisfy is Laplace's equation in cylindrical coordinates. The maximum modulus theorem[4,5] states that if a function satisfied Laplace's equation in a region, then the greatest absolute value of that function occurs on the boundary of the region. Since in this case the value of p_1 is zero at all points of the boundary, it follows from the maximum modulus theorem that p_1 must be zero everywhere inside the boundary. We would have arrived at the same conclusion had we attempted the solution of Equation (18) with the application of boundary conditions (20) and (21).

If p_0 and p_1 are now substituted into Equation (16c), Laplace's equation is again obtained for p_2. Application of Equation (22) and the maximum modulus theorem results in p_2 equal to zero for all z and ω. A progressive application of this procedure results in

$$p_n(z,\omega) = 0$$

and Series (14) becomes

$$p = p_0 = p_g\left(1 - \frac{z}{C}\right) + p_a \tag{23}$$

This result shows that the pressure distribution is independent of ω and the lateral displacement τ, and is linear in z at all

_____

4. R. V. Churchill, <u>Introduction to Complex Variables and Applications</u>, New York, McGraw Hill 1948, p. 95.

5. H. Bateman, <u>Partial Differential Equations of Mathematical Physics</u>, New York, Dover 1944, p. 135.

peripheral points. The pressure at opposite ends of land diameters is the same and results in no net lateral force on the land regardless of the lateral displacement with the restriction that the piston does not contact the wall. This restriction is necessary because the pressure cannot be expressed as an infinite Series (14) which may not converge for $\tau = 1$.

Experimentally we find that no lateral fluid force on the land results when the piston is laterally displaced as shown in Figure (2a). The experimental procedure is described on Page (56) of Chapter VI. This result indicates that the pressure distribution is independent of ω and is given by Equation (23). The pressure gradient is constant and axial in direction in the entire flow region and is equal to - p_g/C. Equation (5a) then states that Q' is directly proportional to the cube of the distance between the flow surfaces or h^3. At peripheral points, ω, where the surfaces are widely separated more fluid flows axially into the flow region than flows in where the surfaces are less widely separated in amounts proportional to h^3, so that the pressure gradient remains the same at all points. Physically then, we can state that if the piston land is out-of-round so that h is a function of ω only (i.e., h is constant in the z direction) the same flow phenomenon occurs and the pressure gradient remains constant and axial

everywhere in the flow region. No lateral force again results for the out-of-round land. However, such a land can contact the bore along a portion of the land and bore surfaces so that the fluid flow is cut off at those points. The pressure distribution existing along the opposite surface of the land holds the land against the bore wall, and for such a case a lateral force results. In considering land and bore configurations it is evident that only the relative configuration is important and that either the land or the bore can give rise to certain geometrical configurations.

We shall now consider the case in which the same piston with circular cylindrical lands is cocked and displaced (i.e., the axial centerline is rotated through an angle γ and displaced laterally a distance of a). This case is shown in Figure (2b). For this piston configuration h is a function of both z and ω and the pressure gradient varies throughout the region of flow. To permit easy mathematical analysis we assume that the flow is predominantly axial, i.e., the axial pressure gradients are much greater than the peripheral pressure gradients. This assumption is good if the axial land length is not great compared to the peripheral length and becomes more valid as the axial length decreases. The errors introduced by such an assumption are discussed in relation to experimental results at the end of

this chapter.

Furthermore, we assume that the axial rotation and lateral displacement occur in the same plane. This assumption is warranted, since we wish to compare analytically and experimentally the magnitude of the lateral force which results from cocking the piston. With such a comparison we can determine the validity of the one-dimensional flow assumption. In Appendix D it is shown that a lateral displacement superimposed on an axial rotation serves only to decrease the lateral force or peripheral pressure gradients. Therefore, the greatest error in assuming the peripheral pressure gradients negligible will occur when the piston is only rotated axially; and from this condition the comparison will yield the most useful results.

Assuming pure axial flow, Equation (6D) of Appendix D yields for the pressure distribution in the flow region,

$$p = P_s - P_g \frac{z\left[1 + (\tau + \gamma\frac{C'}{t} + \gamma\frac{C}{t})\cos\omega\right]^2 \left[2 + 2(\tau + \gamma\frac{C'}{t} + \frac{\gamma}{2}\frac{z}{t})\cos\omega\right]}{c\left[1 + (\tau + \gamma\frac{C'}{t} + \gamma\frac{z}{t})\cos\omega\right]^2 \left[2 + 2(\tau + \gamma\frac{C'}{t} + \frac{\gamma}{2}\frac{C}{t})\cos\omega\right]} \quad (6D)$$

From physical symmetry the component of lateral force in the direction perpendicular to the plane of rotation is zero. The lateral force on one land in the direction of rotation or in the direction of displacement is given as

$$F = \int_0^{2\pi} \int_0^C (pdz)r_0 \cos \omega \, d\omega$$

The derivation of lateral force for this case is given in Appendix D, and Equation (16D) gives the dimensionless lateral force as

$$F_n = \frac{F}{2r_0 C p_g} = \frac{\pi}{(2\tau + 2\gamma \frac{C'}{t} + \gamma \frac{C}{t})^2}\left[\frac{C}{t}\gamma - \frac{2\gamma C}{t\sqrt{4 - (2\tau + 2\gamma \frac{C'}{t} + \gamma \frac{C}{t})^2}}\right]$$

$$(16D)$$

If the piston is of the two land type illustrated in Figure (2b), Equation (16D) is valid for the other land with the difference that T is the negative of τ for the first land. Note that F_n is negative when γ is positive; therefore, the fluid force tends to restore the piston to a position parallel to the bore. If the supply and exhaust pressures are reversed so that the fluid flows toward the center of the piston, the lands will be forced against the wall.

The dimensionless force, $-F_n$, is plotted versus $\frac{\gamma(C + C')}{t}$ for the case of $T = 0$ in Figure (3). The quantity $\frac{\gamma(C + C')}{t}$ is the dimensionless displacement of the end of the piston land. Also plotted in Figure (3) are the experimental results. The procedure used to obtain this data is discussed in Chapter VI. From an inspection of the experimental results we note that the assumption of one-dimensional

DIMENSIONLESS LATERAL FORCE vs. AXIAL ROTATION

(Solution based on assumption of one-dimensional flow)

———— Land of Fig. 2b, Equation(16 D), $\gamma = 0$

△ ▲ Experimental points ($p_g = $ psi, $r_0 = 1.25$ in., $C = 1$ in., $F_n = F/2r_0 p_g C$)
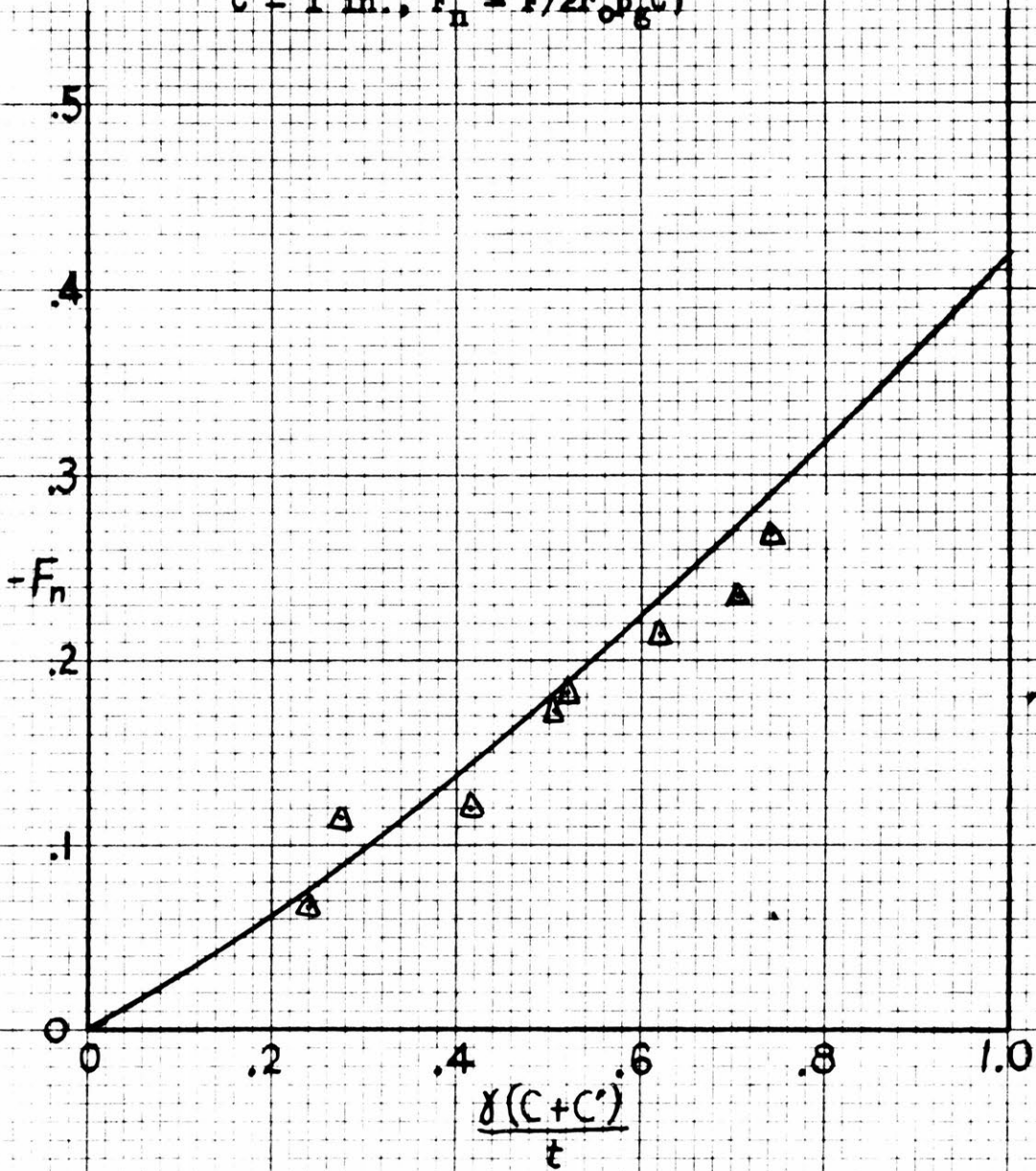
FIG. 3

flow is well warranted, because the mathematical simplification is so great. A more detailed evaluation of the one-dimensional flow assumption is given in Chapter VII after more data is obtained from other piston land shapes.

From the argument of radial symmetry presented on Page (18) of this Chapter the flow at $\omega = 0$ and π must be purely axial; and the pressure distribution found for the assumption of one-dimensional flow must be the true pressure distribution at $\omega = 0$ and π. Therefore, the pressure distribution in the flow region lies within the shaded area of Figure (2b). It is noted that the one-dimensional solution gives the exact pressure distribution along the four boundaries of the flow region and deviates from the true pressure distribution inside the flow region.

CHAPTER IV

RADIALLY STEPPED AND TAPERED LANDS

One method of obtaining a lateral force on a piston land that is displaced from the axial centerline of the bore is to taper or radially step the land (Figure 4). If the taper or step is such that the large radial clearance opens on the high pressure supply, then the lateral force will be in a direction opposite to the displacement or a centering force. For the reverse case the force will be in the direction of displacement.

With an axially imposed pressure drop on the land (Figure 4) and an axial length which is not great compared to the peripheral length we can neglect the peripheral components of the pressure gradient and assume that the flow is purely axial. We will investigate later (Page 36) the average magnitude of the peripheral pressure gradients arising from this assumption.

We can physically see how the centering force obtains when the land is laterally displaced by noting from Equation (1A), Appendix A, that the pressure gradient is inversly proportional to the cube of the gap width (Q' being constant at all axial points for a given ω). For a stepped land, then, the pressure gradients have constant values in the two regions of flow and are related by the inverse ratio of the gap widths cubed or
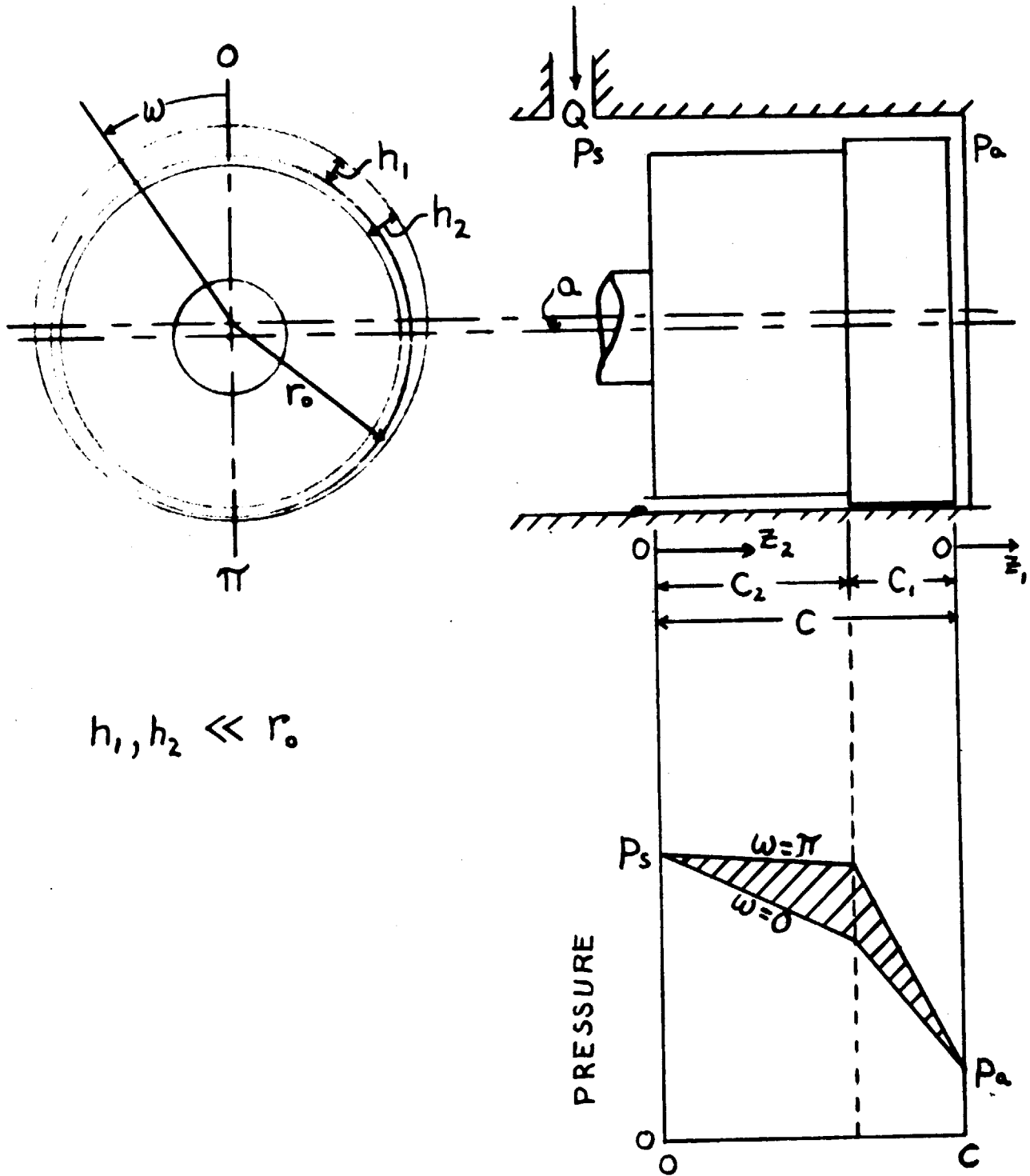
FIG. 4

$$\frac{(dp/dz)_1}{(dp/dz)_2} = \left(\frac{h_2}{h_1}\right)^3 \tag{24}$$

This ratio becomes larger on the side of the piston land which approaches the bore wall and results in a pressure distribution shown in Figure (4).

For convenience we measure the axial coordinate by z_1 in the region of small radial clearance and by z_2 in the region of large radial clearance as shown in Figure (4). Assuming pure axial flow, Equation (3A) of Appendix A gives the pressure distribution in the flow region as

$$p_{z_2} = p_s - \frac{p_g h_1^3 z_2}{C_1 h_2^3 + C_2 h_1^3}$$

$$\tag{3A}$$

$$p_{z_1} = p_a - \frac{p_g h_2^3 z_1}{C_1 h_2^3 + C_2 h_1^3}$$

The lateral force on the land is obtained by integrating the pressure component in the desired direction from $z_2 = 0$ to C_2 and $z_1 = - C_1$ to 0 and then from $\omega = 0$ to 2π. The relationship between C_1, C_2, h_1 and h_2 is obtained in Appendix A by maximizing the rate of change of centering force at zero displacement. The theoretical results were modified as described. Making $(h_2/h_1)_o = 2$, C_1 and C_2 were determined as

$$C_1 = 0.111 \ C$$

$$C_2 = 0.889 \ C$$

The lateral force was then obtained as

$$F_n = \frac{F}{2r_o Cp_g} = \frac{W}{2\tau} \left[0.297 - \frac{0.102}{\sqrt{1.778 - \tau^2}} + \right.$$

$$\left. - \frac{0.510}{\sqrt[4]{1.778 - 1.333 \ \tau^2 + \tau^4}} \sin \left(\frac{\tan^{-1} \frac{2\sqrt{3}}{2 - 3\tau^2}}{2} \right) \right]$$

(12A)

This curve is plotted in Figure (5). The dotted curve shows a similar result for the same overall land dimensions with the step replaced by a uniform axial taper. This latter case was analyzed by J. F. Blackburn.[6] Note that the lateral force for the stepped piston increases much more rapidly than for the conical piston and reaches a maximum value twelve percent greater at the wall.

Note that the pressure distributions shown in Figure (4) are at the peripheral points, $\omega = 0$ and W. At these points the pressure distributions are the same as exist in the actual case of two dimensional flow. They form two boundary conditions imposed on the flow region between

— — — — — — — — — — — — — —

6. Blackburn, J. F., "Lateral Forces on Hydraulic Pistons," Memorandum: DIC 6387, October 5, 1949.
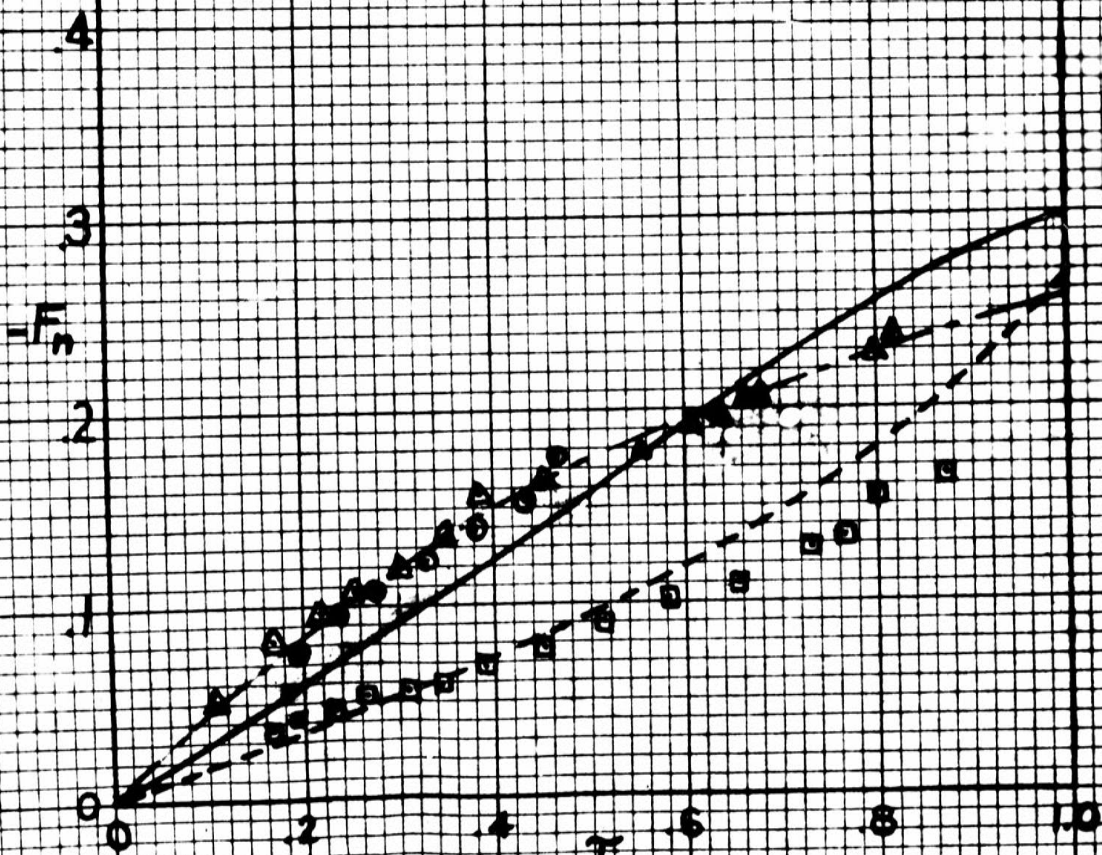
FIG. 5

$\omega = 0$ and π or $-\pi$. That such is the case follows from the argument of radial symmetry presented on Page (18), which shows that at $\omega = 0$ and π the flow and the pressure gradients are purely axial and Equation (1A) is the true flow equation at those two peripheral points. Therefore, because we know the true boundary conditions that the pressure must satisfy on both the axial and peripheral boundaries, we can compare the average peripheral and axial pressure gradients to determine the order of magnitude of the errors introduced by the assumption of pure axial flow everywhere.

The supply pressure, atmospheric pressure, and Equation (3A) of Appendix A give the exact pressure distributions along the following boundaries of the flow region:

$$p(0, \omega)$$
$$p(C, \omega)$$
$$p(z, 0)$$
$$p(z, \pi)$$

The differential Equation (9) that the true pressure distribution must satisfy is elliptic and therefore the pressure at any point in the flow region must be bounded by p_s and p_a.[7] Further, since the pressure must be an even function of ω

_ _ _ _ _ _ _ _ _ _ _ _ _ _

7. Bateman, H., _Partial Differential Equations_, New York, Dover, 1944, pp. 135-138.

and of period 2π (a consequence of the type of argument given on Page 18) it can be expressed as a series of cosine terms. Therefore, at least at $\omega = 0$ and π the pressure must go through a maximum or minimum for any given z. Evidently when τ increases from zero to one (the piston approaches the wall) the pressure at $\omega = 0$ for a given z is a minimum and at $\omega = \pi$ is a maximum. Therefore, the pressure distribution in the flow region lies within the shaded area of Figure (4). We note then that the pressure distribution is a well behaved function in the region of flow varying from a maximum at $\omega = \pi$ to a minimum at $\omega = 0$. Therefore, assuming that a linear peripheral pressure distribution is a close approximation of the actual pressure distribution, we can use the boundary pressures to obtain average values of the peripheral and axial pressure gradients. This procedure should give a good qualitative measure of their relative magnitudes.

The average axial pressure gradient is then - p_g/C and since the pressures at $\omega = 0$ and π are linear in z, the average peripheral pressure drop is just one-half the sum of the maximum and minimum peripheral pressure drops. From an inspection of the shaded area of Figure (4) the average peripheral pressure gradient yields

$$\frac{p_2(C_2, \ 0) - p_2(C_2, \ \pi)}{2\pi r_o} \qquad (25)$$

This gradient is a function of the lateral displacement and is maximum when $\tau = 1$. For $\tau = 1$ and the land dimensions given on Page (70) of Appendix A this average peripheral pressure gradient can be obtained from Equation (3A) by setting either $z_2 = C_2$ or $z_1 = C_1$ since at those values of z the pressures must be equal (Figure 4). This procedure yields for the average peripheral pressure gradient - $p_g/9r_o$. The ratio of this quantity to the average axial pressure gradient then becomes $C/9r_o$. For most commonly designed lands C and r_o are nearly equal (in the experimental piston C = 1 inch and $r_o = 1.25$ inches) and the average peripheral pressure gradients are only one-tenth of the average axial pressure gradients.

From an inspection of Figure (4) it is noted that in the flow region of the larger radial clearance the peripheral pressure gradients are more nearly equal to the axial gradients, and only in the region of smaller radial clearance are the axial pressure gradients actually predominant. Therefore, the overall average ratio of peripheral to axial gradients obtained as one-tenth will be somewhat in error when used to evaluate the validity of the axial flow assumption. However, it is also to be noted that the above found value of one-tenth is computed from the greatest values of peripheral pressure gradients which occur when the land contacts the wall. The average axial pressure gradient on the other

hand remains constant. Therefore, in the curve of lateral
force versus displacement shown in Figure (5) we expect the
actual curve to fall along the curve shown for small values
of displacement and gradually deviate from this curve. At

$\tau = 1$ the error should attain an order of magnitude of about
one-tenth.

The experimental curve shown in Figure (5) increases
more rapidly than expected and gradually falls off with
increasing displacement. At a value of τ equal to 0.6 it
crosses the theoretical curve, reaching maximum deviation
at the bore wall. Percentage-wise the maximum error in
lateral force occurs at small values of displacement where
at some points the theoretical curve falls as much as twenty-
five percent below the experimental curve. This discrepancy
is explained on Page (61) of Chapter VII in a consideration
of the laminar flow transition region. Such a region exists
in all cases where the fluid flows from a large reservoir
with negligible velocity into a small region where the velo-
city is suddenly increased.

The analytical evaluation of the relative magnitu-
des of the average axial and peripheral pressure gradients
discussed above applies exactly to the axially tapered land.
The initial and final clearances of this land are the same
as the stepped land, and the step shown in Figure (4) is
replaced by a uniform axial taper. The true lateral force

for small displacements follows the theoretical curve more closely than does the force for the stepped land. For larger values of displacement the experimental force gradually falls away from the theoretical force reaching maximum deviation at the wall as expected from the above discussion. Better correspondence with theory for the tapered land is due to the smaller effect of the transition to full laminar flow discussed in Chapter VII. In this chapter it is shown that the effects of the transition flow are directly proportional to the flow rate. The flow rate in turn varies as the cube of the clearance between flow surfaces; the average clearance of the tapered land is much less than that of the stepped land where the large clearance extends along 89% of the land ($C_2 = 0.889$, $C_1 = 0.111$). Therefore, the flow rate and the effect of the transition region are much smaller for the tapered land than for the stepped land.

CHAPTER V

PRESSURIZED CYLINDRICAL LAND

Another method of obtaining a lateral force on a
piston land that is displaced from the axial centerline of
the bore involves the pressurized fluid bearing principle;
this is shown schematically in Figure (6). Fluid under a
constant high pressure is supplied so that the fluid flows
through two orifices in series, designated as the upstream
and downstream orifices. The upstream orifice (Figure 6)
is fixed, and the downstream orifice is formed by the land
and bore surfaces. Qualitatively we can see the effect of
changing the downstream orifice by imagining the piston land
to be displaced downward, decreasing the resistance to flow
along the top of the land. As the flow increases the pres-
sure drop in the upstream orifice increases (note Equation
3B) and results in lower pressures at the top of the land.
Similarly the downward displacement of the land increases
the resistance to flow along the bottom of the land, resul-
ting in higher pressures at the bottom of the land. Thus
the downward displacement results in a lateral pressure
force. The pressure distribution along the top and bottom
of the land is shown in Figure (6).

The upstream orifice extends around the periphery
and offers a constant resistance to flow at every ω. (The
orifice is of the capillary type and depends upon the gap

$h, h_1 \ll r_0$
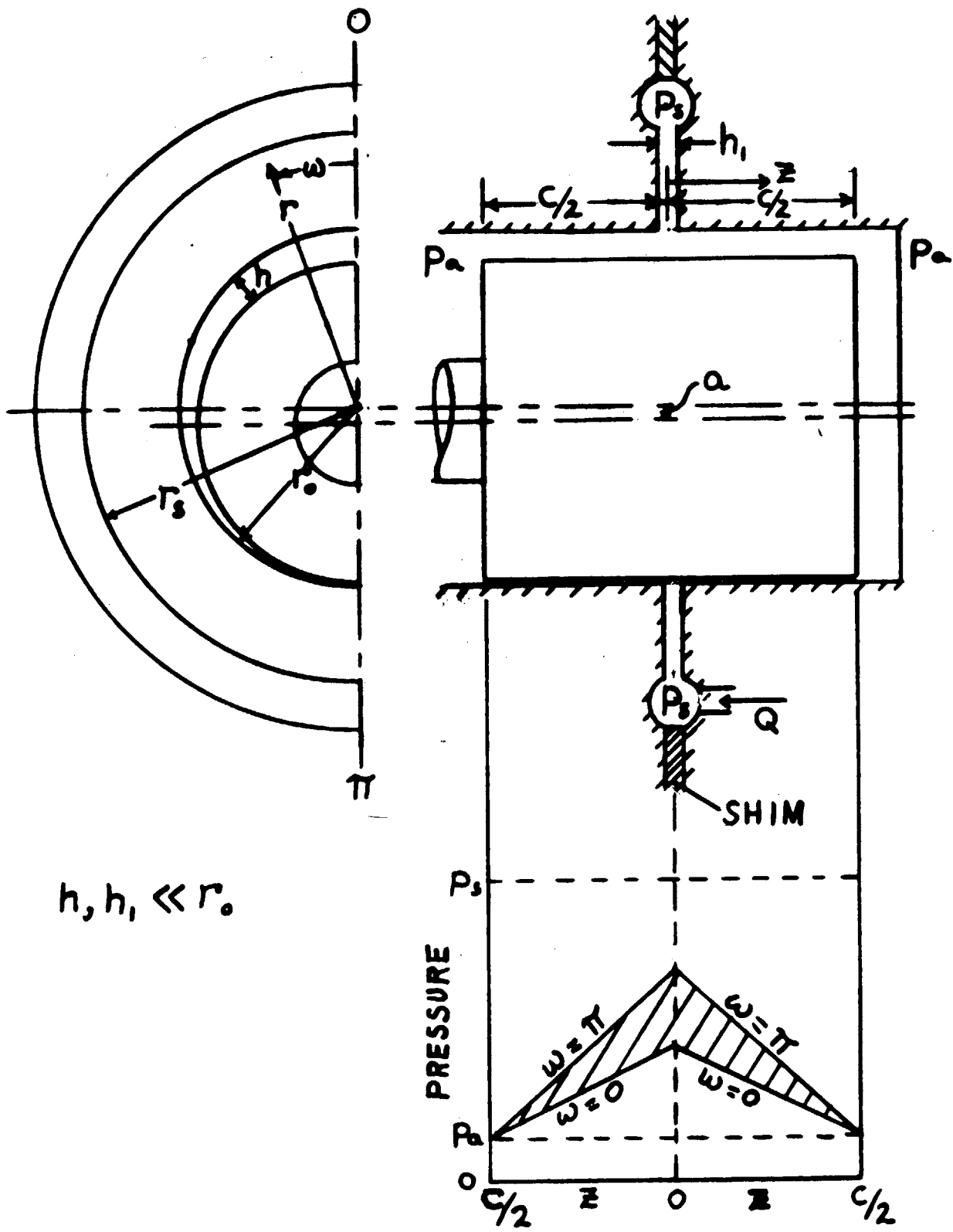
FIG. 6

width between surfaces for its resistance to flow). When
the piston is laterally displaced, the resistance to flow
offered by the downstream orifice varies with ω. For a
downward displacement then every point of the top surface
of the land moves down decreasing the resistance to flow,
and the reverse occurs for the bottom surface. Therefore,
the pressure decreases all over the top surface and increases
over the bottom surface so that a centering force obtains.

The radial and axial flow paths are short compared
to the peripheral paths and the changes in the downstream
gap height produced by a lateral piston displacement are
gradual around the periphery for circular, cylindrical lands
and bores. Therefore, as in the previous cases we assume that
the flow is purely radial in the upstream orifice and purely
axial in the downstream orifice. Appendix B shows that the
pressure distribution in the downstream orifice is given as

$$p_z = p_g \frac{(1 - \frac{2z}{C})}{1 + \frac{4r_o h^3 \ln r_s/r_o}{Ch_1^3}} + p_a \qquad (6B)$$

To obtain the lateral force on the land p_z is inte-
grated with respect to z from $z = 0$ to $C/2$, multiplied by the
cos ω to obtain the component of force in the direction of
displacement, and then the result is integrated again from

$\omega = 0$ to 2π. By physical symmetry about the radial center-line along which the displacement occurs the force in the direction perpendicular to the displacement is zero. Appendix B gives the derivation of the lateral force for the case of the pressurized fluid land; and Equation (13B) gives for the force in the direction of displacement

$$F_n = \frac{\pi}{3\tau} \left[\frac{1}{\sqrt{4 - \tau^2}} - \frac{\cos\left(\dfrac{\tan^{-1}\dfrac{\sqrt{3}}{-1 - 2\tau^2}}{2}\right)}{\sqrt[4]{1 + \tau^2 + \tau^4}} \right] \tag{13B}$$

This dimensionless force is plotted in Figure (7).

Note that the slope of the curve of Figure (7) is greatest at $\tau = 0$. We maximized $-\partial F/\partial \tau$ at $\tau = 0$ with values given by Equation (9B); and from Equation (7A) the maximum value of $-\partial F/\partial \tau$ occurs when $-\partial F'/\partial h$ is a maximum at every ω. The quantity $-\partial F'/\partial h$ is a function of h and is a maximum for only one value of h; and therefore h must be independent of ω for Equation (7A), Appendix B, to yield a maximum for $-\partial F/\partial \tau$. Only at $\tau = 0$ is h independent of ω (piston land centered). Since we have maximized $-\partial F/\partial \tau$ at $\tau = 0$, the greatest slope of Figure (7) occurs at the origin.[7]

_ _ _ _ _ _ _ _ _ _ _ _ _ _ _

7. Note that $-\partial F/\partial \tau$ can be maximized at different values of τ which would give a slope that is maximum for a particular τ but which is less than the absolute maximum at $\tau = 0$.

DIMENSIONLESS LATERAL FORCE vs. DISPLACEMENT

(Pressurized fluid land Fig. 6)

———— Equation (13 B) based on assumption of one-dimensional flow

- - - - Exact two-dimensional solution, good for small values of γ where terms of order γ^2 and higher are neglected in series of type Equation (14); (Ref. 6)

Slope: 0.564

Initial slope: 0.588
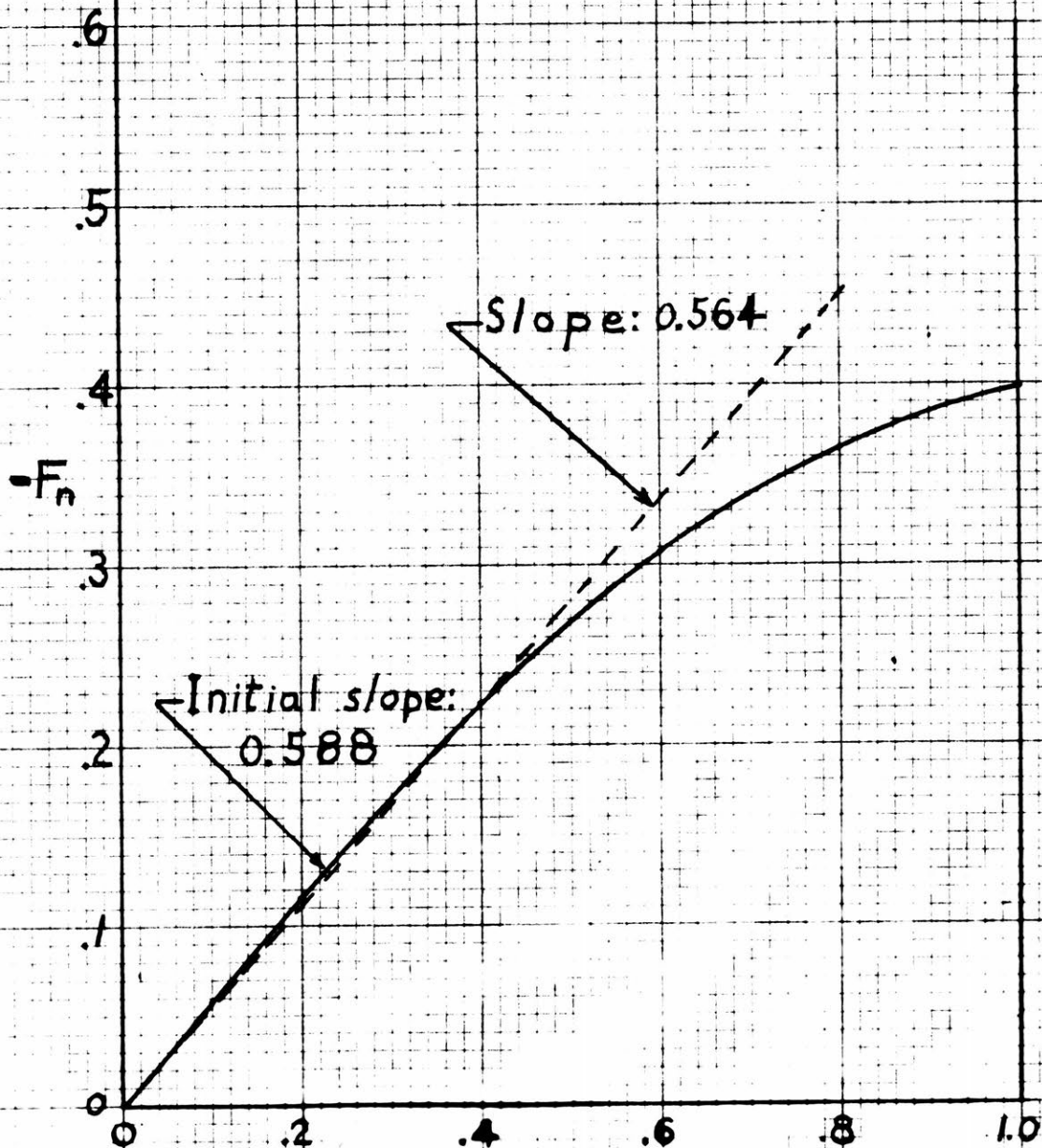
FIG. 7

From the argument of radial symmetry about the center-
line $\omega = 0$ (Page 18) the actual pressure distribution must be
an even and periodic function of ω and can be expressed as a
series of cosine terms. This implies that the pressure for
a given z must be maximum or minimum at least at $\omega = 0$ and π
and that the peripheral pressure gradient is then zero at
those two values of ω. Therefore, the flow at $\omega = 0$ and π
must be purely axial and the pressure distributions there
are the same as those that obtain at $\omega = 0$ and π from the
assumption of one dimensional flow everywhere. Evidently
from an inspection of Figure (6) the pressure distribution at

$\omega = 0$ must be a minimum and at $\omega = \pi$ a maximum along the land
surface, and the pressure distribution at any other ω in the
region of flow must lie within these values or in the shaded
area of Figure (6) determined by the amount of lateral dis-
placement. We see then that the one-dimensional solution
satisfies the boundary conditions of the exact solution and
deviates in the interior of the flow region.

It is of interest to check the error in the lateral
force introduced by the assumption of pure axial flow (i.e.,
neglecting pressure gradients in the peripheral direction).
The exact two-dimensional solution for lateral force for
small displacements was solved at the Instrumentation Labora-
tory, M.I.T.[8] The solution was obtained by a series type

---

8. Instrumentation Laboratory, "The Pressurized Fluid Bearing
   for High Precision Instrument Suspension," Cambridge,
   Massachusetts, 1948, pp. 93-94.

expansion as Equation (14) in this paper in which all terms of higher degree than τ were neglected. This solution, however, will give the exact initial slope of the curve of lateral force versus displacement or $(-dF_n/d\tau)_0$. For the optimum length dimensions determined in Appendix B by Equation (9B) the exact two dimensional solution gives

$$-\left(\frac{dF_n}{d\tau}\right)_0 = 0.564$$

Equations (7A and 8B) can easily be evaluated at $\tau = 0$ and give for the assumption of pure axial flow for the same land and bore geometry the result

$$-\left(\frac{dF_n}{d\tau}\right)_0 = 0.588$$

This last result is less than five percent greater than the actual rate of increase of lateral force. Since the error between the actual force and the force obtained with the assumption of negligible peripheral pressure gradients is so small, the assumption of predominantly axial flow must be good to the extent of the error introduced in the lateral force, or five percent error. This error holds at least for small displacements. For larger values of lateral piston displacement the rates of change of peripheral pressure gradients must become smaller, because the rate of change of

lateral force depends directly upon them;[9] and from Figure
(7) we note that this rate of change becomes smaller with
increasing displacement. We expect that the true curve of
Figure (7) will follow closely the one-dimensional curve
shown for small displacements and gradually deviate, reach-
ing maximum deviation at the wall.

- - - - - - - - - - - - - - - - - -

9. An inspection of Equations (7B, 7A and 8B) of Appendix
    B illustrates the relationship.

CHAPTER VI

TEST EQUIPMENT AND EXPERIMENTAL METHODS

The test equipment consisted in the main of a large
ten to one scale piston model. The piston was of the simple
two land type with oil under pressure supplied between the
lands as shown in Figures (2a, 2b, 4, and 6). The piston
dimensions shown were as follows:

$$C = 1.00 \text{ inches}$$
$$2C' = 0.75 \text{ inches}$$
$$C_1 = 0.111 \text{ inches}$$
$$C_2 = 0.889 \text{ inches}$$
$$r_0 = 1.25 \text{ inches}$$
$$t = 0.003 \text{ inches}$$

The main body with the piston bore was of three piece construc-
tion and pinned. This construction was employed to enable
tests to be made using the pressurized fluid land, shim stock
separating the three pieces as shown in Figure (6).

The oil used was the same as that used with the pro-
totype piston. To maintain dynamic similarity as discussed in
Chapter I the pressure was reduced by a factor of one hundred
and supplied at twenty or twenty-five pounds per square inch
from a hydraulic test stand. The entire test equipment[11] is

---
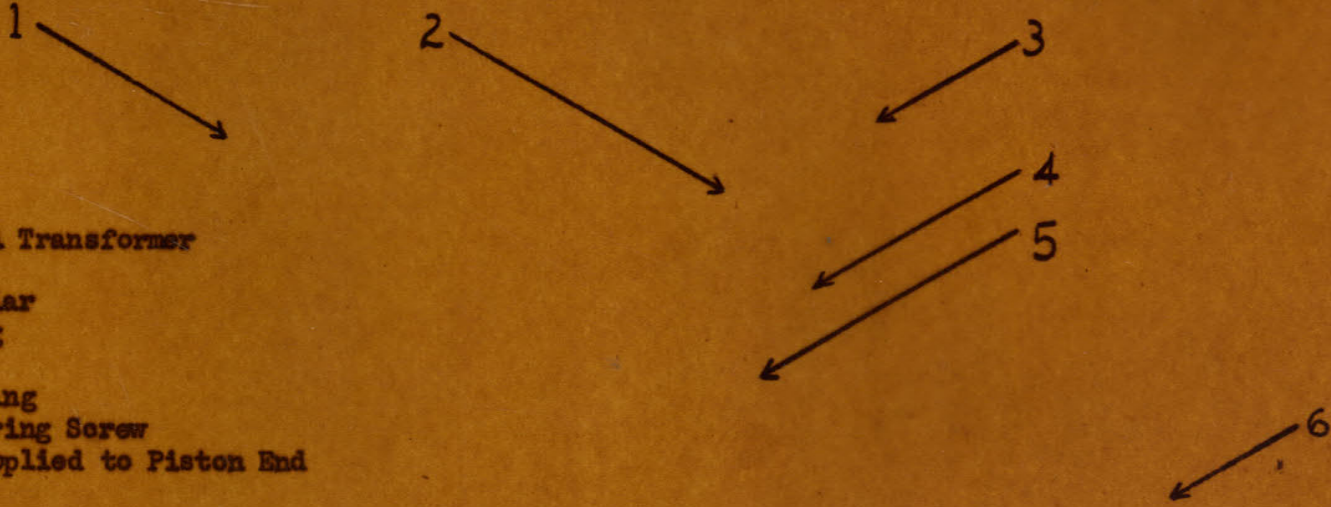
11. Shop drawings of the parts are obtainable at the Dynamic
   Analysis and Control Laboratory, M.I.T. Drawing Nos.
   D-11094-AY, C-11094-1, A-11094-2 through A-11094-7,
   C-11094-8, C-11094-9, and B-11094-10.
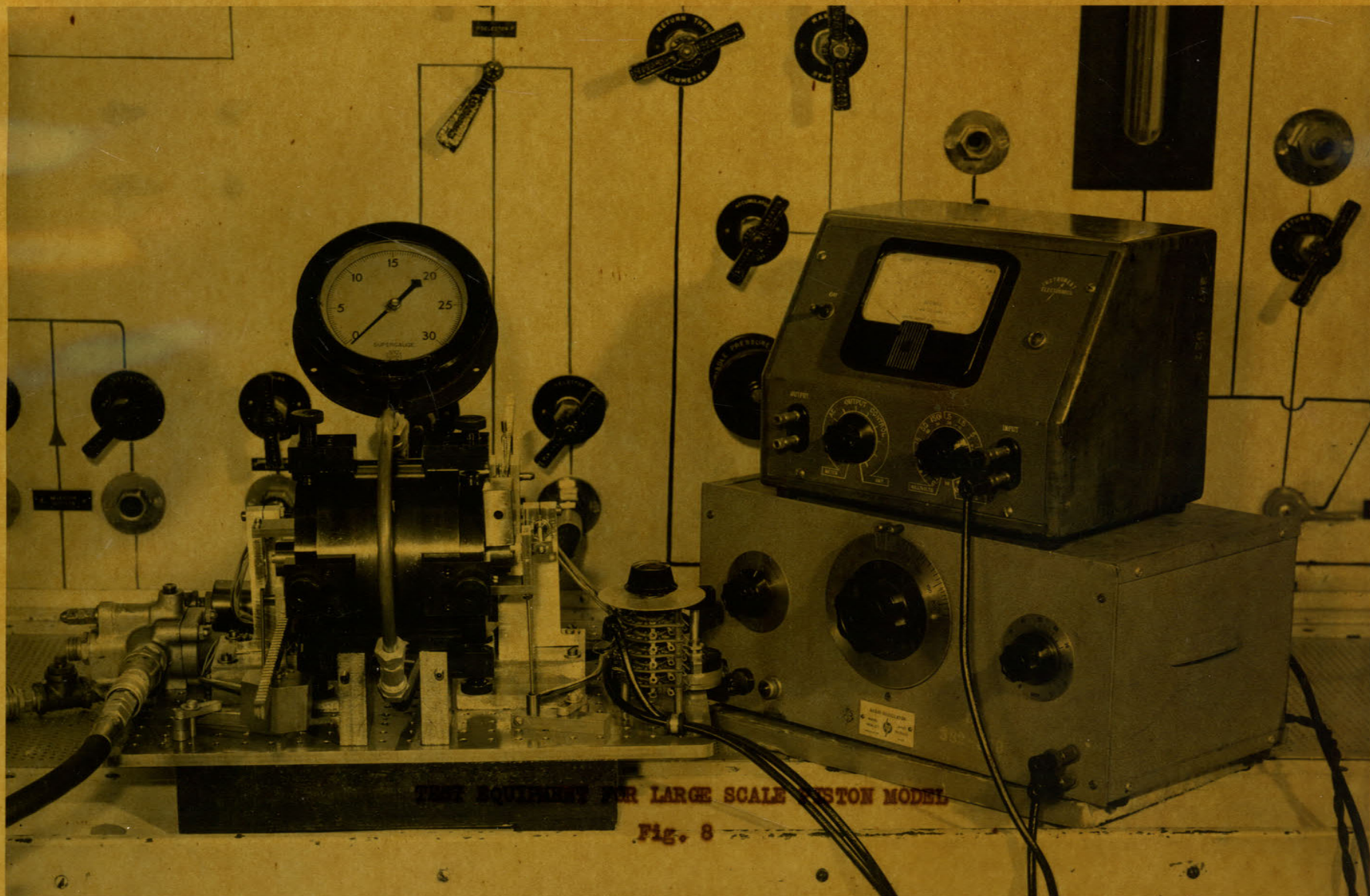
TEST EQUIPMENT FOR LARGE SCALE PISTON MODEL

Fig. 8
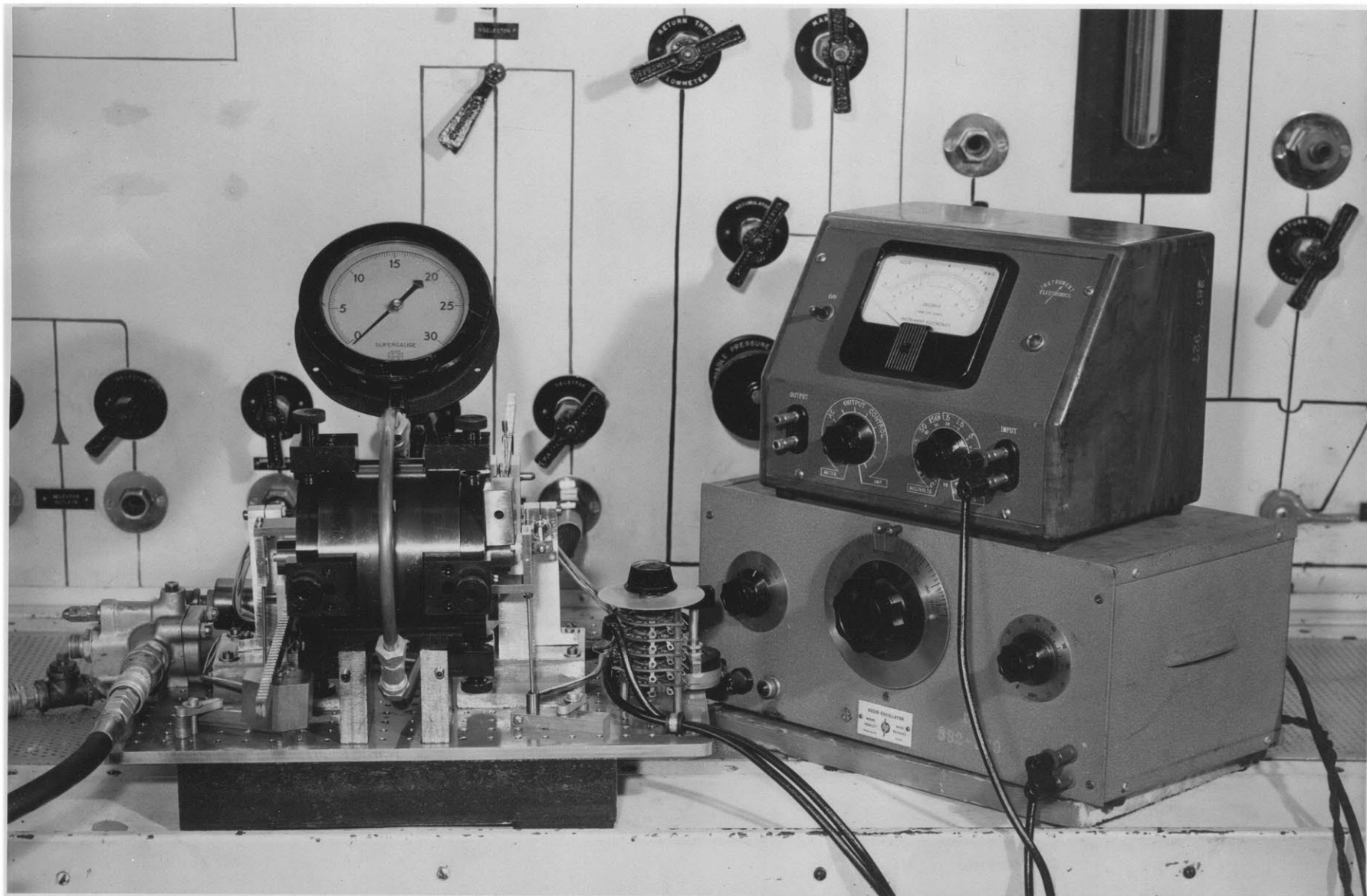
1. Linear Differential Transformer
   (Linearsyn)
2. Piston Support Collar
3. Spring Support Ring
4. Piston
5. Piston Support Spring
6. Differential Centering Screw
7. Lever and Weight applied to Piston End

END VIEW OF LARGE SCALE PISTON MODEL

Fig. 9
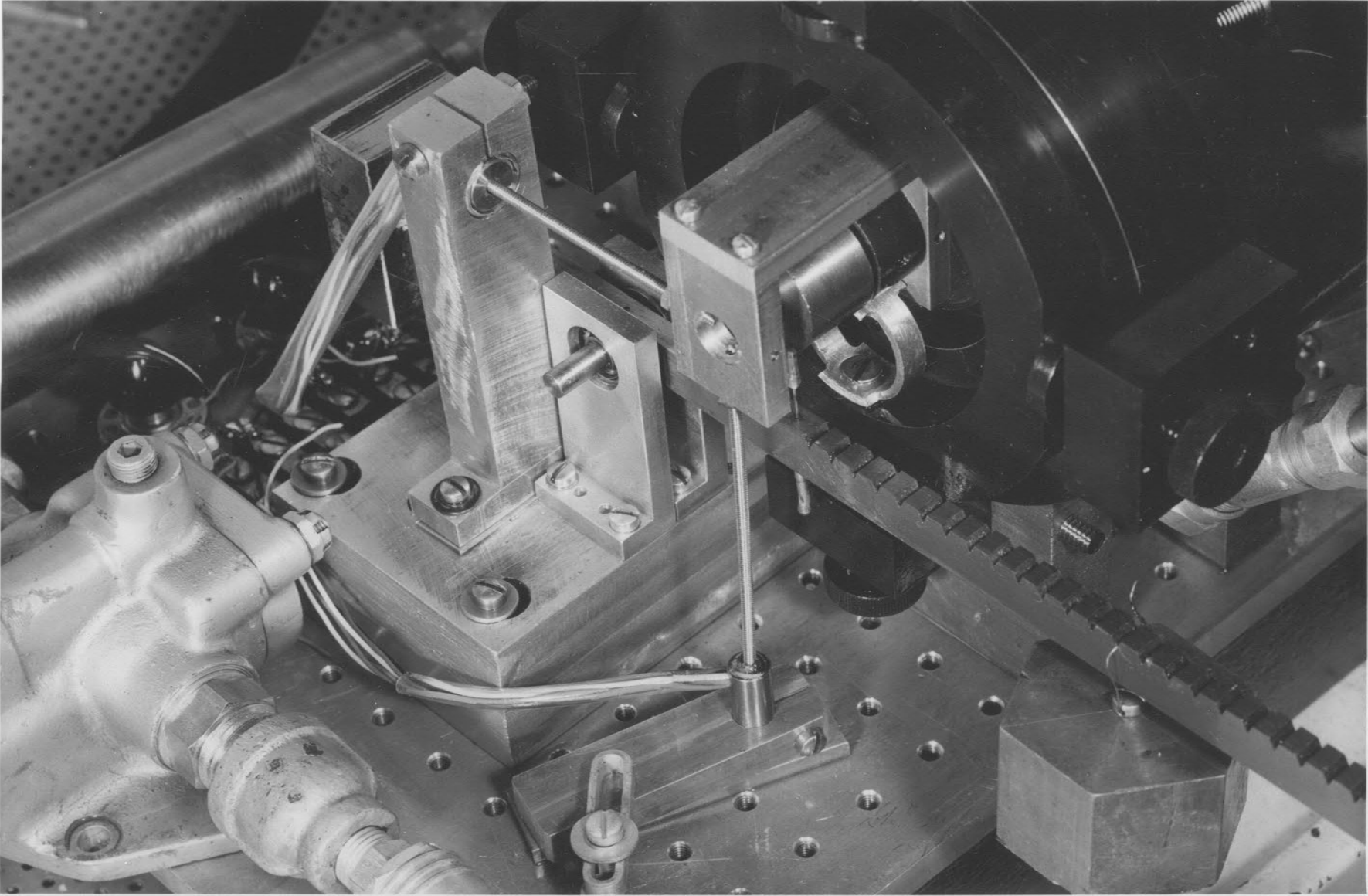
shown in Figures (8 and 9), and the following description
of the experimental procedure can be easily followed by
reference to those figures.

To measure the lateral force exerted by the fluid
on a piston land stiff springs (thin-walled rings) between
the piston and the main body were calibrated for lateral
force and displacement. The springs were designed for a
theoretical spring constant of about 7000 pounds per inch.
Linear differential transformers (Linearsyns) were used to
measure the displacement and calibrate the springs.

First, the Linearsyns were calibrated for displace-
ment versus voltage output using a ten-thousandth's dial indi-
cator and an Instrument Electronics Voltmeter. An ordinary
oscillator furnished the excitation voltage of five volts
at five thousand cycles per second. A typical curve resulting
is shown in Figure (10), giving a sensitivity of twenty milli-
volts per one-thousandth of an inch displacement.

The Linearsyns were then installed with the equip-
ment as shown in Figure (9) with the iron slugs mounted to
the piston and the transformer coils mounted on the base or
stationary part of the equipment. To center the piston
laterally the large spring support ring to which the springs
were mounted was moved vertically at one end of the piston
by the differential screws while the extremes of travel were
measured by the output voltage of the Linearsyns. When the

LINEARSYN OUTPUT VOLTAGE vs. DISPLACEMENT
(Excitation voltage of 5 volts at
5000 cps, null of 0.6 millivolts)

Displacement (inches x 10³)
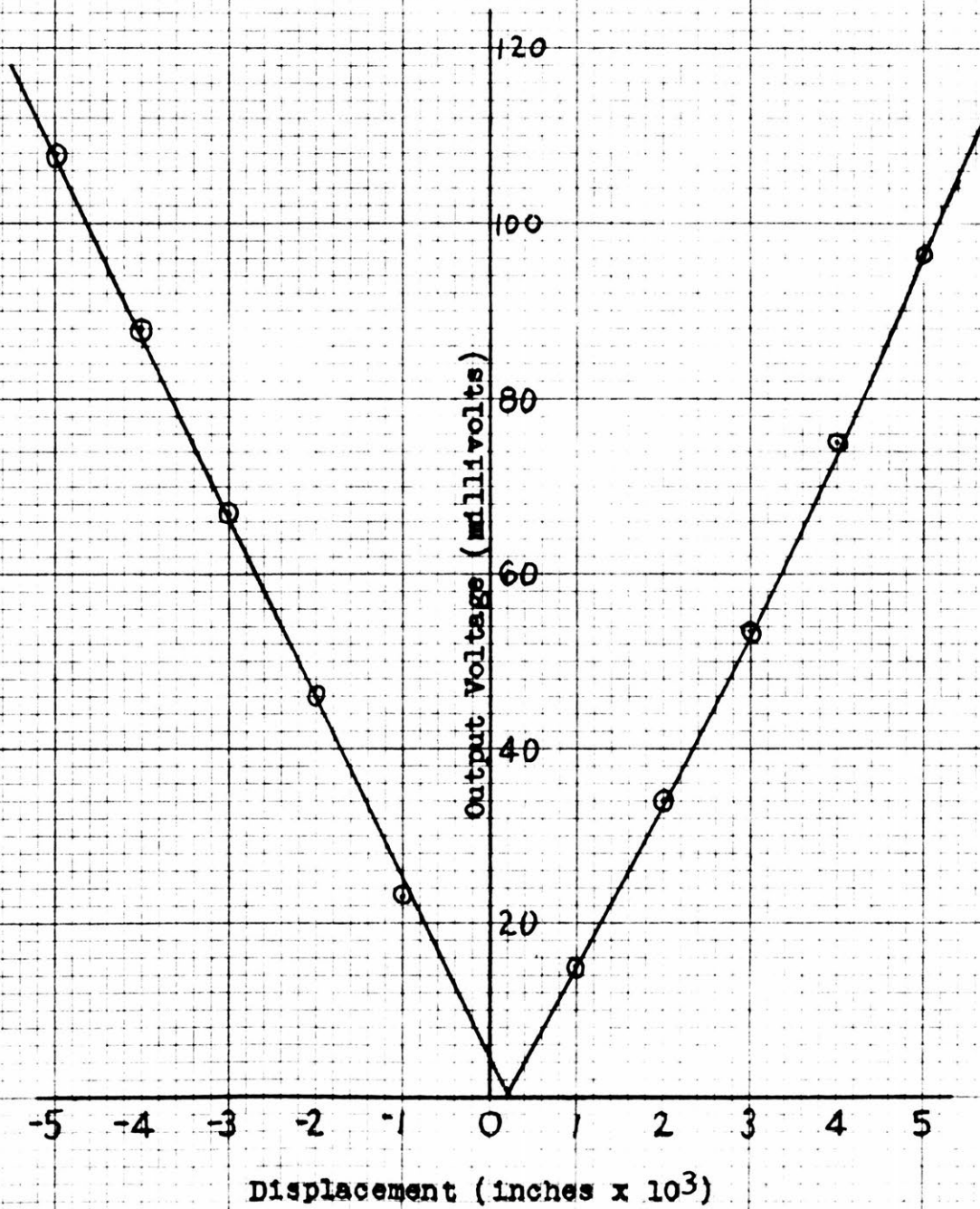
FIG. 10

piston land reached the wall, the voltage output remained constant while any further movement of the large ring served only to compress the springs. Since the curve of voltage output versus displacement, Figure (9), was linear, the center position of the piston was the arithmetic mean of the extreme voltages. This procedure was repeated in the horizontal direction and then again repeated for the vertical and horizontal directions at the other end of the piston. With a few trials the piston was perfectly centered.

The Linearsyns and spring combinations were next calibrated for force and voltage output by hanging known weights on the levers shown in Figure (9). This procedure resulted in a curve of force versus output voltage, or by virtue of the calibration curve of displacement versus voltage, the curve was transformed to a curve of force versus displacement. For the case of the stepped land oil under a pressure of twenty pounds per square inch was then supplied between the lands as shown in Figure (4), and another curve of force versus displacement was obtained in the way described. Two typical curves are shown in Figure (11). The force due to the fluid pressure distribution is the difference between the two curves at each value of displacement, because at a given displacement the net force is always represented on the calibration curve. The force exerted by the fluid on the stepped lands, when laterally

FORCE APPLIED TO PISTON END vs.
LINEARSYN OUTPUT VOLTAGE or LATERAL DISPLACEMENT
(Land of Fig. 4, $p_g = 20$ psi, $r_o = 1.25$ in.,
$C = 1.000$ in., $C_1 = .111$ in., $C_2 = .889$ in.)
Wall contacted at 65 millivolts
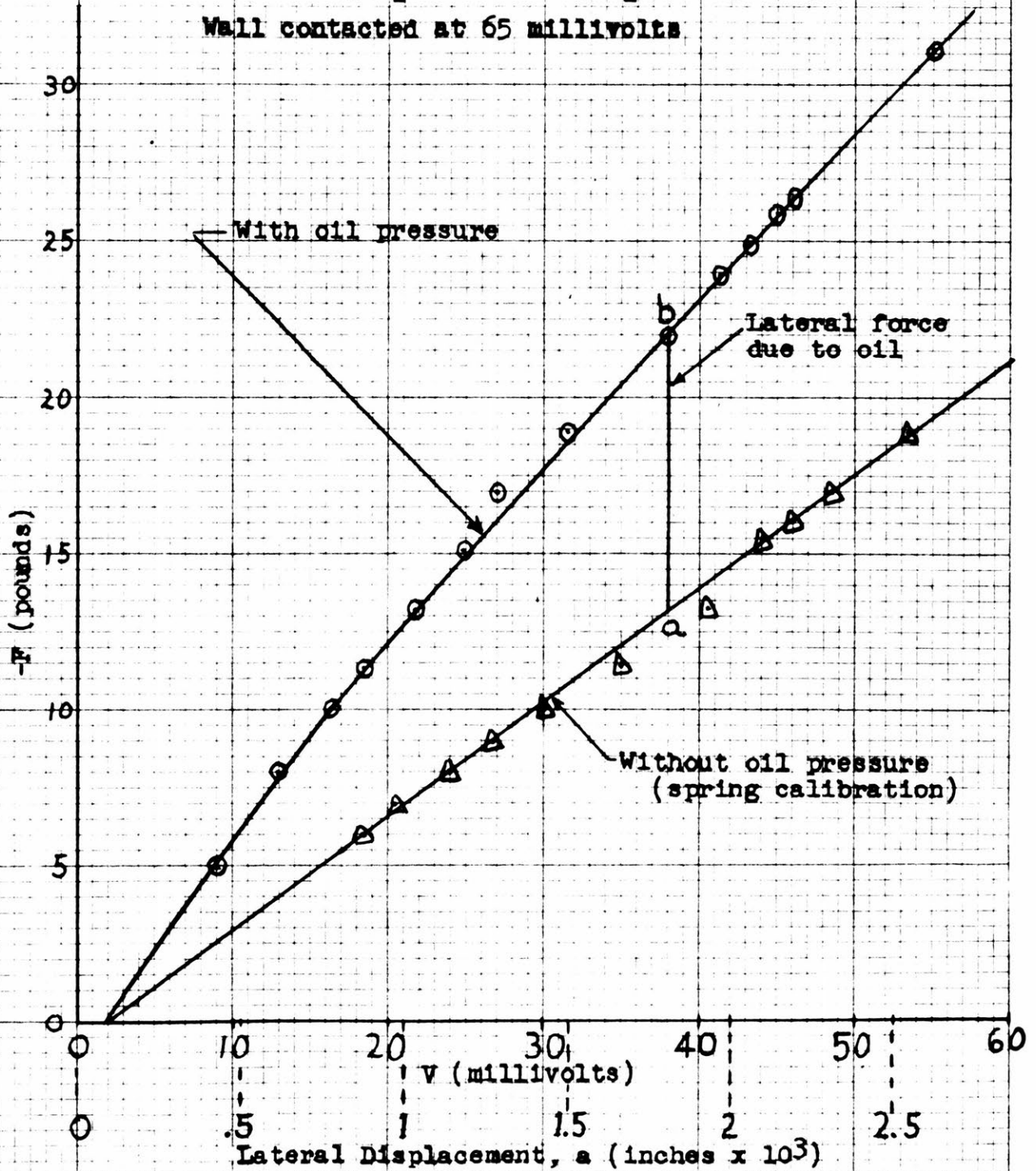
FIG. 11

displaced, is of the same magnitude and direction for either land and is given directly for one land by a line such as ab of Figure (11).

This difference in the force curves represents a force at the point of application of the weights; therefore, for the case of the Figure (2b) where the piston has only an axial rotation γ (a = 0), this force becomes a moment balanced by the moment due to the fluid pressure on the land. After an inspection of the pressure distribution resulting from a cocked piston (Equation 6D), it was assumed that the center of pressure was located approximately at the center of the axial land length. (Actually it starts from that point at $\gamma = 0$ and moves slowly in the direction of increasing z as γ increases). Then from the dimensions of the piston the forces on the lands acted at points 1.75 inches apart. The weights were applied to the piston six inches apart, and the fluid force was obtained by equating moments. Force rather than moment was obtained for comparison to Equation (16D) or Figure (3), which gives force as a function of the axial rotation γ and the displacement τ (τ is zero in Figure 3).

After calibration of the springs and Linearsyns for force and displacement, an alternative method of measuring lateral force was employed. Using the differential screws, the piston was laterally displaced a known

amount (given by voltage output of Linearsyns). Then the oil was supplied under pressure, and if the leakage fluid exerted a lateral force, the piston was further displaced due to a compression or expansion of the springs. Since the springs were calibrated, the displacement gave the lateral force exerted by the fluid. The additional displacement caused by this force was used to correct the original lateral displacement.

The method just discussed was employed to verify the conclusions of Chapter III, which stated that if a circular cylindrical land (Figure 2a) is displaced laterally, no force results. However, this method of measuring lateral force does not yield accurate results when a lateral force obtains, because the springs in general exert both a force and a bending moment on the piston. The moment is dependent on the way the large spring supporting ring is clamped by the differential screws; moving the ring to a new displacement may alter this moment and change the spring calibration for force. The first method described circumvents this difficulty since the ring remains clamped during the experimental runs. The two force-displacement curves of Figure (11) are obtained by hanging weights on the ends of the piston once without oil supplied and then with the oil supplied. In this case the bending moment exerted by the springs, although indeterminate, remains the same at a given

displacement, and the difference in force between the two curves is due only to the fluid.

Experimental results for the land types shown in Figures (2b and 4) are plotted in Figures (3 and 5) respectively.

CHAPTER VII

EVALUATION OF RESULTS AND VALIDITY OF
ONE-DIMENSIONAL FLOW ASSUMPTION

To evaluate the validity of the theoretical results
we shall employ experimental data obtained for lateral force
and displacement for the straight cylindrical land shown in
Figures (2a and 2b), the stepped land shown in Figure (4), and
the tapered land. The experimental results for these lands
are plotted in Figures (3 and 5). All the theoretical results
are obtained from the assumption of pure axial, laminar flow
(i.e., peripheral pressure gradients are neglected). Analyti-
cally the average peripheral pressure gradients are about one-
tenth of the axial pressure gradients, and we expect good
results from the analysis based on pure axial flow. The experi-
mental points in Figure (3) for the cocked circular cylindrical
land fall very near the theoretical curve substantiating the
results expected.

Figure (5) shows the experimental points for the
radially stepped land. These points indicate that the lateral
force increases more rapidly than the theoretical force for
small values of displacement. It gradually drops off, crossing
the theoretical curve at τ equal to 0.6, reaching maximum
deviation at the wall.

The greater initial rate of increase of lateral
force may find explanation in a consideration of the transi-
tion region of laminar flow. When fluid flows from the large
supply reservoir into the small region of flow, a certain
length of the flow region is necessary to fully develop the

laminar velocity profile. See Figure (12). As the fluid enters the region of flow, its velocity is uniform across the clearance separating the surfaces. At the surfaces the fluid becomes stationary, and the viscous action of the fluid begins to decrease the velocity of adjoining fluid layers; gradually more and more of the fluid is affected in a region beginning at the surfaces and extending inward toward the center of the clearance space. The same amount of fluid flows into the transition region as flows out; therefore, since the velocity near the surfaces decreases from the initial uniform velocity, the layers of fluid near the center of the flow region must be accelerated to a higher velocity. This acceleration of the inner fluid layers occurs at the expense of a pressure drop which is in addition to the laminar flow pressure drop. For flow in pipes the transition region is found to vary from twenty to fifty diameters, depending upon the flow rate and entrance section. The length of the transition region is greater if the entrance region has a sharp corner, which causes eddies in the flow.

In the case of the stepped land the radial clearance is 0.006 inches in the entrance region which begins in a sharp corner. If flow in a pipe is used as an indication, the transition region could extend a length of 0.300 inches along the axial land length, whose total length is only one inch. When the land is displaced downward, more fluid flows
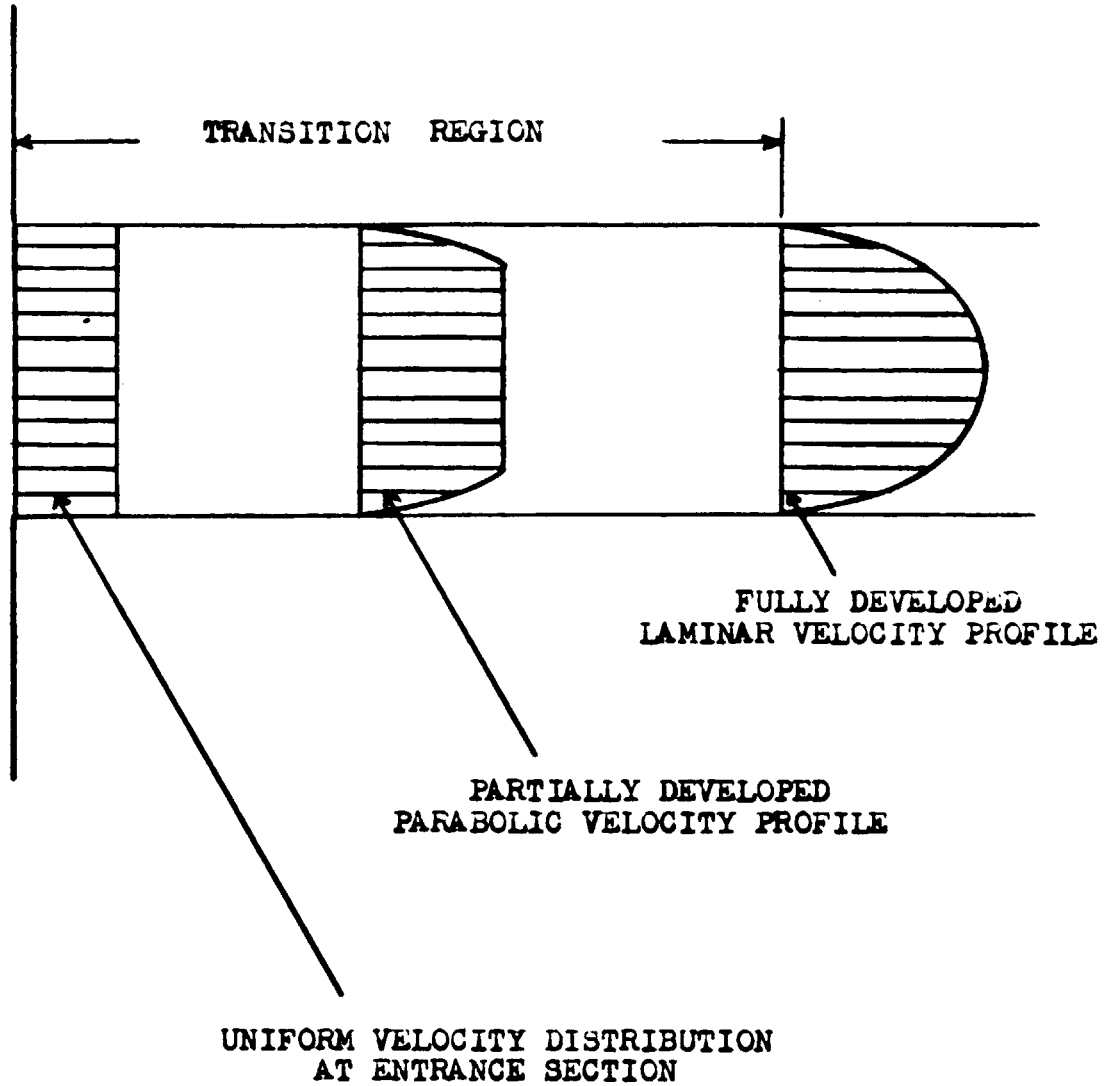
TRANSITION LENGTH TO FULL LAMINAR FLOW

FOR FLOW FROM LARGE RESERVOIR INTO SMALL CROSS-SECTION

FIG. 12

into the region along the top of the land and less along the bottom. A greater initial pressure drop occurs along the top of the land, because more fluid must be accelerated in developing the laminar flow profile. The pressures along the top surface of the land become smaller and a still larger lateral force results than is indicated by the assumption of complete laminar flow everywhere.

The phenomenon just described was not measurable for the straight, cylindrical land of Figure (2a), because the radial clearance was only half as great. Since flow varies as the cube of the gap width, the flow for the straight land was only one-eighth of the flow for the stepped land. The additional pressure drop in the transition region,and, therefore, the lateral force is proportional to the flow rate. The experimental results for the straight land with smaller radial clearance plotted in Figure (3), therefore, fall nearer the theoretical curve.

Although the theoretical lateral force deviates as much as twenty-five percent at some points from the actual force, the assumption of one-dimensional laminar flow is well warranted in consideration of the great mathematical simplification resulting. Neglecting the laminar flow transition region, Figure (7) illustrates for the pressurized fluid land the small error between the exact two-dimensional solution and the one-dimensional solution for

small values of displacement.

Note that for all three land types considered the orders of magnitude of the lateral forces resulting are same. From the dimensional analysis presented in Chapter I the force on the prototype piston is the same as that on the large scale model. For conventional land dimensions and a pressure drop of 2000 psi for the prototype piston (20 psi for the model) this force attains a value of about fifteen pounds. The dry friction force resulting from such a lateral force on an improperly designed land can become very large.

All dimensions of the model piston are ten times as large as those of the prototype, and the step on the land of Figure (4) becomes 0.0003 inches on the prototype land. In grinding a theoretically straight land a taper of this magnitude could result; and as shown in Appendix A, a tapered or stepped land with the small radial clearance opening toward a high pressure region will cause a decentering force. In view of such a possibility it may be desirable to design stepped lands which would always result in a centering force. A step is much easier to machine or grind and gives rise to a greater centering force than the tapered land. See Figure (5).

High spots on a land can be qualitatively analyzed through the stepped land. A high spot is essentially a step, changing the pressure gradient as shown in Figure (5). From

an inspection of the pressure distribution shown in this figure it is noted that a centering or decentering force due to the pressure distribution can result depending upon the location of the high spot. If a high spot on one side of a land is nearer the high pressure region, the land will be forced against the bore wall by the linear pressure distribution existing on the opposite side of the land. However, if the high spot is nearer the low pressure region, the land will locate itself so that the pressure distribution resulting will be balanced by the linear pressure distribution on the opposite side of the land.

A consideration of high spots on the land leads to the possibility that dirt particles in the fluid may cause a lateral force which will force the piston land against the wall. Dirt particles that are carried into the flow region may cause silting near the entrance region. Although not completely cutting off the flow of oil, they may cause a large pressure drop near the entrance region, lowering the pressure downstream on one side of the land. The pressure distribution on the opposite side of the land forces the land and dirt particles against the wall. The lateral force resulting from the silting of dirt particles may attain a value as large as that resulting on a stepped or tapered land.

In Chapter III it was shown that no lateral force results on a straight circular, cylindrical land that is

only laterally displaced. This result was extended to show that no lateral force results on a displaced out-of-round land if the out-of-round condition is uniform in the axial direction. However, an out-of-round land can contact the bore wall along a portion of the land and bore surfaces, cutting off the flow (no fluid pressure distribution). The pressure distribution existing on the opposite side of the piston land will hold it against the wall; and for this one condition a lateral force will result on a straight landed piston.

From the preceding discussion on land taper, land high spots and out-of-round lands it is seen that the prototype piston land with radial clearances of 0.0002 inches and less is a very delicate object, and great care must be taken in manufacture. This is especially true if the piston is to be used with a low axial force level stroking mechanism as in many control applications. In this paper we have endeavored to analyze the lateral forces resulting from certain land and bore configurations in order to permit more efficient land designs by eliminating as much as possible dry friction resulting from lateral fluid leakage forces.

APPENDIX A

DERIVATION OF EQUATION FOR LATERAL FORCE
ON A STEPPED DIAMETER LAND

One piston land shape that will give rise to a lateral force when displaced from the axial centerline is that of a stepped land subjected to two different but uniform pressures over each axial end as in Figure 3. As the product of the land length, C, and the radial clearance becomes very small compared to the diameter or peripheral length, then the flow becomes predominantly axial. Therefore, if we assume pure axial capillary flow between two surfaces with a small separation the flow Equation (5) becomes

$$\frac{dp}{dz} = -\frac{12\,\mu}{h^3}\, Q'$$ (1A)

Solutions of this equation give the pressure distribution over the surface of the land as a function of z, and h, or as a function of z and ω because h is some other function of z and ω. The resulting pressure distribution can be integrated over the surface of the land to obtain the lateral fluid force.

Integration of Equation (1A) gives

$$p_s - p_{z_2} = \frac{12\,\mu\,z_2}{h_2^{\,3}}\, Q'$$

$$p_{z_1} - p_a = - \frac{12 \mu z_1}{h_1^3} Q' \tag{2A}$$

where z_1 and z_2 are measured as shown in Figure (4).

Inserting the boundary condition that at $z_2 = C_2$ and $z_1 = -C_1$, $p_{c_2} = p_{c_1}$ and eliminating Q' the pressure distribution in the two regions of flow becomes

$$p_{z_2} = p_s - \frac{p_g h_1^3 z_2}{C_1 h_2^3 + C_2 h_1^3}$$

$$\tag{3A}$$

$$p_{z_1} = p_a - \frac{p_g h_2^3 z_1}{C_1 h_2^3 + C_2 h_1^3}$$

The force per unit peripheral width exerted by the fluid pressure on the land is obtained by integrating p_{z_2} from 0 to C_2 and p_{z_1} from $-C_1$ to 0.

$$F' = \frac{p_g}{2} \frac{(C_1^2 + 2C_2 C_1) h_2^3 + C_2^2 h_1^3}{C_1 h_2^3 + C_2 h_1^3} + p_a C \tag{4A}$$

The total fluid force exerted on the land (positive in the direction of piston displacement, a, from the axial centerline) is obtained by integrating the component of pressure force in the direction of the displacement. By symmetry the fluid force perpendicular to this direction is zero, and

the total force on the land in the direction of the displace-
ment is

$$F = \int_0^{2\pi} F' \cos \omega \, r_o \, d\omega \qquad (5A)$$

Also from symmetry, or realizing that the integral
of the $\cos \omega$ from 0 to 2π is 0, the force on the land is zero
when the piston is centered with respect to the bore. When
the piston is laterally displaced, h_1 and h_2 are functions of
ω; and for small values of the ratio of radial clearance to
the land radius are given as an excellent approximation by

$$h_1 = t(1 + \tau \cos \omega)$$
$$\qquad (6A)$$
$$h_2 = e + t(1 + \tau \cos \omega)$$

where t = radial clearance at large land diameter and

$$\tau = \frac{a}{t}$$

Before evaluating the lateral force, it is desir-
able that some optimum condition be satisfied by the force,
since it is a function of C_2/C_1 and h_2/h_1. The purpose of
obtaining a centering force on the piston is to keep the land
from contacting the wall, resulting in static friction rather
than fluid friction. Two obvious possibilities are to maxi-
mize the centering force when the piston is in contact with

the wall, or to maximize the rate of change of centering force with displacement at zero displacement. The first involves the evaluation of an integral and much more algebraic manipulation than the latter. Consequently the method of maximizing the rate of change of lateral force with displacement at zero displacement will be employed. Note that to obtain a centering force (i.e., opposite to the lateral displacement) the rate of change of centering force with displacement must be the negative of the rate of change of lateral force which through our choice of coordinates acts in the direction of displacement. Hence, for a centering force $(-\frac{\partial F}{\partial \tau})$ must be positive.

The derivative of Equation (5A) with respect to displacement is:

$$-\frac{\partial F}{\partial \tau} = -\int_{0}^{2\pi} \frac{\partial F'}{\partial \tau} \cos \omega \; r_0 d\omega$$

$$\frac{\partial F'}{\partial \tau} = \frac{\partial F'}{\partial h} \frac{dh}{d\tau}$$

From the geometry of Figure (3) or Equation (6A),

$$\frac{dh}{d\tau} = t \cos \omega; \text{ and } dh = dh_1 - dh_2$$

Therefore

$$-\frac{\partial F}{\partial \tau} = \int_{0}^{2\pi} -\frac{\partial F'}{\partial h_1} tr_0 \cos^2 \omega \, d\omega \qquad (7A)$$

At the centerline h_1, h_2 and $\frac{\partial F'}{\partial h_1}$ are independent of ω and $(-\frac{\partial F}{\partial \tau})_0$ can be maximized by maximizing $(-\frac{\partial F'}{\partial h_1})_0$. Writing first that $h_2 = h_1 + e$ and $C_2 = C - C_1$, we obtain from the derivative of Equation (4) the result

$$-\left(\frac{F'}{h_1}\right)_0 = \left\{\frac{3p_g C}{2} \frac{C_1(C-C_1)(1 + \frac{e}{h_1})^2(\frac{e}{h_1^2})}{\left[C_1(1+\frac{e}{h_1})^3 + C-C_1\right]^2}\right\}_0 \qquad (8A)$$

Note that the right hand member of Equation (8A) is negative when $e = h_2 - h_1$ is positive, and is positive when e is negative. Therefore, the fluid will exert a centering force on the land if the boundary pressures are such that fluid flows from the region of large to small clearance and will exert a decentering force if the boundary pressures are reversed.

To maximize the rate of change of centering force the derivatives of $\left(-\frac{\partial F'}{\partial h_1}\right)_0$ are taken with respect to e and C_1 and equated to zero. This procedure obtains the results:

$$C_1 = \frac{C}{1 + \left(\frac{h_2}{h_1}\right)_0^3} \qquad \text{and} \qquad \begin{array}{c} e = h_{20} \\ h_{10} = 0 \end{array}$$

That these values give a maximum rather than a minimum can be seen by noting that all length dimensions must be positive, and then that $-\frac{\partial F'}{\partial h_1} \geqslant 0$. Since the above obtained values result in a value of $-\frac{\partial F'}{\partial h_1}$ which is greater than zero, they

must give a maximum. This can also be checked by trying various values of C_1 and $(h_2/h_1)_o$ as C_1 approaches zero and $(h_2/h_1)_o$ approaches ∞.

Evidently h_{1o} cannot be set at zero; but for a given h_{1o}, making $(h_2/h_1)_o$ as large as possible within the limitations of capillary axial flow, C_1 for the optimum condition can be determined from Equation (8A). The entire flow analysis presented here assumes capillary and axial flow. As the clearances between piston land and cylinder increase, both assumptions become less valid; and therefore h_{2o} cannot be increased indefinitely to obtain large values of $(h_2/h_1)_o$. Furthermore, the minimum radial clearance necessary for free piston movement commensurate with grinding accuracies obtainable is about 0.0002 inches for the prototype piston land, giving a value of 0.002 inches for the ten to one scale model. For such a value of h_{1o} setting h_{2o} at 0.004 inches or $(h_2/h_1)_o = 2$ is about as large a value as would be warranted under the flow assumptions made.

From Equations (8 and 5a) and $(h_2/h_1)_o = 2$,

$$C_1 = 0.111 \ C$$

$$C_2 = 0.889 \ C$$

$$h_1 = t(1 + \tau \cos \omega)$$

$$h_2 = t(2 + \tau \cos \omega)$$

Substituting these values into Equations (4A and 5A), the force exerted by the fluid on the land is

$$F = \frac{p_g r_o C}{2} \int_o^{2\pi} \frac{0.210(2+\tau\cos\omega)^3 + 0.790(1+\tau\cos\omega)^3}{0.111(2+\tau\cos\omega)^3 + 0.889(1+\tau\cos\omega)^3} \cos\omega\, d\omega +$$

$$(10A)$$

$$+ p_a r_o C \int_o^{2\pi} \cos\omega\, d\omega$$

The second integral is zero and the first is most easily integrated by Cauchy's integral or residue integration.[12] Appendix C gives the derivation for evaluating integrals of the form

$$\int_o^{2\pi} \frac{d\omega}{re^{i\sigma} + k\cos\omega} \qquad (1C)$$

with the restriction that the integrand remain finite for all real values of ω. Integrals arising from axial capillary flow in an eccentric annulus for any piston shape or configuration can be reduced by division and partial fraction expansion to the form above.

– – – – – – – – – – – – – – – –

12. R. V. Churchill, Complex Variables and Applications, pp. 90-92, 125-134.

By division to reduce the degree of the numerator in Equation (10A) to one less than the degree of the denominator we obtain

$$F = \frac{p_g r_o C}{C} \int_0^{2\pi} \left[\cos \omega + \frac{0.297}{\tau} + \right.$$

$$\left. - \frac{0.100 \, \tau^2 \cos^2 \omega + 0.494 \, \tau \cos \omega + 0.520}{(\tau \cos \omega + 1.333)(\tau \cos \omega - \frac{2}{\sqrt{3}} e^{15\pi/6})(\tau \cos \omega - \frac{2}{\sqrt{3}} e^{-15\pi/6})} \right] d\omega \tag{11A}$$

The first term integrates to zero, and a partial fraction expansion gives

$$F = \frac{p_g r_o C}{2\tau} \int_0^{2\pi} \left[0.297 - \frac{0.102}{1.333 + \tau \cos\omega} + \right.$$

$$\left. + \frac{i \, 0.255}{\frac{2}{\sqrt{3}} e^{-i\pi/6} + \tau \cos \omega} - \frac{i \, 0.255}{\frac{2}{\sqrt{3}} e^{i\pi/6} + \tau \cos \omega} \right] d\omega$$

τ is a dimensionless displacement parameter given by 5a where $0 \leqslant \tau \leqslant 1$. The restriction placed on Equation (1C) is satisfied (i.e., all integrands remain finite for all real values of ω), and Equation (11A) now is integrable by ordinary

methods and the use of Equation (3C) of Appendix C. Each
separate term of Equation (11A) may yield a complex number,
but the force must be real and the sum of the integrated
terms must yield a real number. This fact serves as a check
on the evaluation of real integrals by the method of complex
residue integration. Application of Equation (3C) Appendix
C yields

$$\frac{F}{2r_o C p_g} = \frac{\pi}{2\tau} \left[0.297 - \frac{0.102}{\sqrt{1.778 - \tau^2}} + \right.$$

$$\left. - \frac{0.510}{\sqrt[4]{\frac{16}{9} - \frac{4}{3} \tau^2 + \tau^4}} \sin\left(\frac{\tan^{-1}\frac{2\sqrt{3}}{2 - 3\tau^2}}{2}\right) \right] \tag{12A}$$

The dimensionless force coefficient $F/2r_o C p_g$ is formed for
convenience in comparison with other land shapes and confi-
gurations and is plotted versus dimensionless displacement,
τ, in Figure (5).

An infinite number of curves of force versus dis-
placement can be found for the infinite number of combina-
tions of C_1 and $(h_2/h_1)_o$. However, since

$$-\frac{\partial F}{\partial \tau} = \int_0^{2\pi} - \frac{\partial F'}{\partial h_1} t\, r_o \cos^2\omega\, d\omega$$

$- \partial F/\partial \tau$ can have its absolute maximum[13] only when $- \partial F'/\partial h_1$ is an absolute maximum for every ω. This must occur at zero displacement, because only at that point are the values of C_1, h_2/h_1, and $- \partial F'/\partial h_1$ which obtain a maximum, the same at every ω or peripheral point. Alternatively, since $- \partial F'/\partial h_1$ must be a maximum for every ω, it cannot be a function of ω; and the point of zero displacement from the axial centerline is the only point which satisfied that condition. In Figure (5) the slope at the origin is not the greatest value obtainable, because the optimizing dimensions given on Page (69) were modified due to the physical limitations on the dimensions.

---

13. Absolute maximum refers to a maximum with respect to both C_1 and h_2/h_1. For any particular value of h_2/h_1, C_1 can be found to obtain a maximum value of $\partial F'/\partial h_1$ which may not be the value of h_2/h_1 for an absolute maximum.

APPENDIX B

DERIVATION OF LATERAL FORCE ON A CIRCULAR,
CYLINDRICAL LAND AS A PRESSURIZED FLUID BEARING

The geometry of the pressurized fluid land is shown in Figure (4). If the flow in the upstream capillary orifice is assumed radial and the flow along the surface of the land is assumed axial,[14] we can write for the pressure gradients in the upstream and downstream orifices from Equations (5) that

$$\frac{dp}{dr} = \frac{12\mu}{h_1{}^3} Q' = \frac{12\mu}{h_1{}^3} \frac{dQ}{rd\omega} \tag{1B}$$

$$\frac{dp}{dz} = -\frac{12\mu}{h^3} \frac{Q'}{2} = -\frac{6\mu}{h^3} \frac{dQ}{r_0 d\omega} \tag{2B}$$

The factor of one-half occurs in Equation (2B) since the flow divides at the center of the land surface and flows out in opposite axial directions. The flow per unit width, Q', in Equation (1B) is a function of r and must be taken into account when integrating to obtain the pressure distribution. Upon integration of Equation (1B) from p_s to p_r and Equation (2B) from p_z to p_a we obtain

$$p_s - p_r = \frac{12\mu \, dQ}{h_1{}^3 \, d\omega} \ln \frac{r_s}{r} \tag{3B}$$

----

14. The validity of these assumptions is discussed on Page (45).

$$p_z - p_a = \frac{6\mu}{h^3 r_o} \frac{dQ}{d\omega} \left(\frac{C}{2} - z\right) \tag{4B}$$

The pressure p_r at $r = r_o$ is equal to the pressure p_z at

$z = 0$. By inserting this condition into Equations (3B) and

(4B) we can solve for $dQ/d\omega$.

$$\frac{dQ}{d\omega} = \frac{p_g h_1^3 h^3 r_o}{3\mu \left(Ch_1^3 + 4r_o h^3 \ln r_s/r_o\right)} \tag{5B}$$

Substituting this expression back into Equation (4B) yields

$$p_z = p_g \frac{\left(1 - \frac{2z}{C}\right)}{1 + \frac{4r_o h^3 \ln r_s/r_o}{Ch_1^3}} + p_a \tag{6B}$$

The lateral force per unit peripheral width of land

(taking into account both halves of the land) is given as

$$F' = 2 \int_o^{C/2} p_z dz = \frac{p_g C/2}{1 + \frac{4h^3 r_o \ln r_s/r_o}{Ch_1^3}} + p_a C \tag{7B}$$

and the total lateral force on the land is

$$F = \int_o^{2\pi} F' \cos \omega \, r_o d\omega \tag{5A}$$

Again as discussed on Page (67) we shall maximize the negative
rate of change of F with displacement at zero displacement.
The negative is taken, because -F corresponds to a centering
force. The derivative of Equation (5A) is given on Page (68)
as

$$(-\frac{\partial F}{\partial \mathcal{T}}) = \int_0^{2\pi} (-\frac{\partial F'}{\partial h}) \, t \, r_0 \cos^2\omega \, d\omega \tag{7A}$$

This equation can be maximized at zero displacement by maxi-
mizing $(-\partial F'/\partial h)_0$ because at the centerline h and $(-\partial F'/\partial h)$
are independent of ω. The derivative of Equation (7B) is

$$-\frac{\partial F'}{\partial h} = \frac{6p_g r_0 C^2 h_1^3 h^2 \ln r_s/r_0}{(Ch_1^3 + 4r_0 h^3 \ln r_s/r_0)^2} \tag{8B}$$

For zero displacement h is equal to the radial clearance and
the variables in Equation (8B) are h_1 (the gap width of the
upstream orifice) and r_s (the radius to the supply pressure
groove). See Figure (4).

To maximize $(-\partial F/\partial h)_0$ with respect to both h_1 and
r_s we take their respective partial derivatives and equate
them to zero. This procedure yields for both resulting
equations

$$\frac{4r_0 h^3}{Ch_1^3} \ln r_s/r_0 = 1 \tag{9B}$$

Note that h_1 is determined only as a function of r_s. This result could have been anticipated upon consideration of the fact that the pressure drop in the orifice depends both upon r_s and h_1; and the same pressure drop can be obtained for different combinations of r_s and h_1. At zero displacement or the centered position ($h = t$) the condition that will result in the greatest slope of the curve of centering force versus displacement becomes from Equation (9B)

$$\frac{4r_o t^3}{Ch_1^3} \ln \frac{r_s}{r_o} = 1 \tag{10B}$$

and F' from Equation (7B) becomes

$$F' = p_g \frac{C/2}{1 + h^3/t^3} + p_a C \tag{11B}$$

Inserting F' and h from Equations (11B) and (6A) into (5A) yields

$$F = \frac{Cr_o p_g}{2} \int_0^{2\pi} \frac{\cos \omega \, d\omega}{1 + (1 + \tau \cos \omega)^3} \tag{12B}$$

This equation is again of the form given in Appendix C by Equation (1C). Following the procedure outlined there we can expand the integrand by a partial fraction expansion which yields

$$F = \frac{Cr_oP_g}{2} \int_0^{2\pi} \left[-\frac{\frac{2}{3\tau}}{\tau \cos \omega + 2} + \frac{\frac{1}{3\tau}}{\tau \cos \omega + e^{-i\pi/3}} + \frac{\frac{1}{3\tau}}{\tau \cos \omega + e^{i\pi/3}} \right] d\omega$$

Using Equation (3C) we can evaluate the separate terms in this integral and obtain

$$F = \frac{Cr_oP_g}{2} 2\pi i \left[-\frac{2}{3\tau i \sqrt{4 - \tau^2}} + \frac{1}{3\tau i \sqrt[4]{1 + \tau^2 + \tau^4}} (e^{i\alpha/2} + e^{-i\alpha/2}) \right]$$

where

$$\alpha = \tan^{-1} \frac{\sqrt{3}}{-1 - 2\tau^2}$$

This can be further simplified to give the following form

$$F_n = \frac{-F}{2r_o C p_g} = \frac{\pi}{3\tau} \left[\frac{1}{\sqrt{4 - \tau^2}} + - \frac{\cos\left(\frac{\tan^{-1} \frac{\sqrt{3}}{-1 - 2\tau^2}}{2}\right)}{\sqrt[4]{1 + \tau^2 + \tau^4}} \right] \quad (13B)$$

The left hand member of Equation (13B) is plotted versus τ in Figure (7).

APPENDIX C

EVALUATION OF INTEGRALS BY RESIDUE INTEGRATION

Capillary fluid flow in an eccentric annulus in which the flow is predominantly perpendicular to the plane of the annulus, i.e. pressure gradients in the axial direction are much greater than those in the peripheral direction, give rise to integrals of the form

$$\int_0^{2\pi} f(\sin \omega, \cos \omega) \, d\omega$$

Residue integration[15] in the complex plane can be employed for evaluation of such integrals if f is a rational function of $\sin \omega$ and $\cos \omega$ and if f remains finite for all real values of ω.

In particular by virtue of the capillary flow equation

$$\frac{dp}{dz} = -\frac{12\mu}{h^3} Q',$$

where h is the radial width of the annulus and Q' is the axial flow rate per unit peripheral length, we arrive at integrals

---

15. Churchill, R. V., Complex Variable and Applications, pp. 90-92, 125-134.

which can be expressed by partial fraction expansion as a sum of terms of the type

$$I = \int_0^{2\pi} \frac{d\omega}{re^{i\sigma} + k \cos \omega} \qquad (1C)$$

If we consider ω as the argument of the complex number z on the unit circle $z = e^{i\omega}$, we can write

$$\cos \omega = \frac{z^2 + 1}{2z}, \quad d\omega = \frac{dz}{iz}$$

Equation (1A) becomes by Cauchy's residue theorem

$$I = \int_c f(z)dz = \int_c \frac{2dz}{ik(z^2 + 2\frac{r}{k}e^{i\sigma}z + 1)} = \qquad (2C)$$

$$2\pi i \sum (\text{Residues inside } c)$$

where c is the unit circle $|z| = 1$. The poles of $f(z)$ occur at values of z for which

$$z^2 + 2\frac{r}{k}e^{i\sigma}z + 1 = 0,$$

or at

$$z_{1,2} = \frac{1}{k}\left[- re^{i\sigma} + (r^4 - 2r^2k^2 \cos 2\sigma + k^4)^{\frac{1}{4}} e^{\frac{1}{2}(\alpha + 2n\pi)}\right]$$

where

$$\alpha = \tan^{-1}(\frac{\sin 2\sigma}{\cos 2\sigma - k^2/r^2}); \quad n = 0, 1$$

Of the two poles only one lies inside the unit circle because their product $(z_1 \cdot z_2)$ must equal one by Equation (2C). By inspection the pole inside the unit circle is

$$z_1 = \frac{1}{k} \left[- re^{i\sigma} + (r^4 - 2r^2k^2\cos 2\sigma + k^4)^{\frac{1}{4}} e^{\frac{i\alpha}{2}} \right]$$

The residue at z_1 for the case of simple poles is

$$\text{Res}_{z_1} = \left[(z - z_1) f(z) \right]_{z = z_1}$$

$$= \frac{1}{i(r^4 - 2r^2k^2 \cos 2\sigma + k^4)^{\frac{1}{4}} e^{\frac{i\alpha}{2}}}$$

Hence from Equation (2C),

$$I = \int_0^{2\pi} \frac{d\omega}{re^{i\sigma} + k \cos\omega} = 2\pi i \sum (\text{Residues inside } c)$$

$$= \frac{2\pi}{(r^4 - 2r^2k^2\cos 2\sigma + k^4)^{\frac{1}{4}} e^{\frac{i\alpha}{2}}} \tag{3C}$$

where $\alpha = \tan^{-1} \frac{\sin 2\sigma}{\cos 2\sigma - k^2/r^2}$

APPENDIX D

DERIVATION OF LATERAL FORCE ON A COCKED
AND DISPLACED CIRCULAR CYLINDRICAL LAND

If a right circular, cylindrical land becomes cocked and displaced (i.e., axial centerlines of piston land and bore are rotated and displaced with respect to each other, Figure 2b) a moment exerted by the fluid results tending to restore the piston land to a position parallel to the bore. To enable easy mathematical treatment we will assume that the flow is predominantly axial, i.e., the peripheral pressure gradients are negligible compared to the axial pressure gradients. This assumption is good if the axial land length is not great compared to the peripheral length. The errors introduced by such an assumption are discussed analytically later with respect to other types of land geometry. Further it is assumed that the axial rotation and lateral displacement occur in the same plane. At the end of this Appendix it is shown that displacement in any direction serves only to reduce the lateral force on a land.

With the assumption of pure axial flow we can use Equation (5) to obtain the pressure distribution in the flow region. Inspection of Figure (2b) yields for the radial gap height

$$h = t \left[1 + \left(\tau + \gamma \frac{C'}{t} + \gamma \frac{z}{t} \right) \cos \omega \right] \qquad (1D)$$

where τ and γ are positive for downward displacement and clock-wise rotation respectively. The limits on γ can be found by noting that the displacement of the end of the piston land is limited by the radial clearance, or an inspection of Figure (2b) yields

$$0 \leqslant |a| + |\gamma (c' + c)| \leqslant t$$

$$\text{or} \quad 0 \leqslant |\tau| + \left| \gamma \frac{(c' + c)}{t} \right| \leqslant 1 \tag{2D}$$

Equation (5) becomes for pure axial flow at any given

$$\int_{p_s}^{p} dp = - \frac{12\mu \, Q'}{t^3} \int_{o}^{z} \frac{dz}{\left[1 + (\tau + \gamma \frac{c'}{t} + \gamma \frac{z}{t}) \cos \omega \right]^3} \tag{3D}$$

To make writing more compact we can make the following temporary substitutions:

$$m = 1 + (\tau + \gamma \frac{c'}{t}) \cos \omega$$

$$e = \frac{\gamma}{t} \cos \omega$$

Equation (3D) becomes:

$$\int_{p_s}^{p} dp = - \frac{12\mu \, Q'}{t^3} \int_{o}^{z} \frac{dz}{(m + ez)^3} \tag{4D}$$

The integration of this equation yields

$$p - p_s = \frac{6\mu Q'}{t^3 e} \frac{m^2 - (m + ez)^2}{m^2(m + ez)^2} \tag{5D}$$

By using the boundary condition that at $z = C$, $p = p_a$ we can solve for Q' and substitute back into Equation (5D) which gives the pressure distribution in the region of flow as

$$p = p_s - \frac{p_g(m + eC)^2 \left[m^2 - (m + ez)^2\right]}{(m + ez)^2 \left[m^2 - (m + eC)^2\right]} \tag{6D}$$

Integrating for the moment exerted by the fluid on the entire piston becomes cumbersome, and therefore we will find the lateral force on a single land and assume that the center of pressure acts at the center of the axial land length. Inspection of the resulting pressure distribution (Equation 6D) will show that this point is a satisfactory approximation.

The force per unit peripheral width is given as

$$F' = \int_0^C p \, dz \tag{7D}$$

Substitution of Equation (6D) yields an equation which is again easily integrable, and we obtain

$$F' = p_s C + p_g \frac{(m + eC) \, C^2 e}{m^2 - (m + eC)^2} \tag{8D}$$

This equation can be simplified by substituting for p_s its equivalent $p_g + p_a$; then resubstituting the values for g and e yields

$$F' = p_a C + p_g C \frac{1 + (\tau + \gamma \frac{C'}{t}) \cos \omega}{2 + (2\tau + 2\gamma \frac{C'}{t} + \gamma \frac{C}{t}) \cos \omega} \qquad (9D)$$

The component of lateral force in the direction perpendicular to the displacement is zero by symmetry and the component of this force in the direction of displacement is given as

$$F = \int_0^{2\pi} F' \cos \omega \, r_0 d\omega$$

and by substituting Equation (9D)

$$F = C r_0 \int_0^{2\pi} p_a \cos \omega \, d\omega + p_g \frac{\cos \omega + (\tau + \gamma \frac{C'}{t}) \cos^2 \omega}{2 + (2\tau + 2\gamma \frac{C'}{t} + \gamma \frac{C}{t}) \cos \omega} \, d\omega$$

$$(10D)$$

The first term of this equation integrates to zero. Again we can write this equation more compactly with the following substitutions:

$$a' = 2\tau + 2\gamma \frac{C'}{t} + \gamma \frac{C}{t}$$

$$(11D)$$

$$b' = \tau + \gamma \frac{C'}{t}$$

And Equation (10D) becomes

$$F = p_g C r_o \int_0^{2\pi} \frac{\cos \omega \, d\omega}{2 + a' \cos \omega} + \frac{b' \cos^2 \omega \, d\omega}{2 + a' \cos \omega} \qquad (12D)$$

Now if we divide the numerators by the denominators in Equation (12D), we can reduce the integrand to the type of terms given by Equation (1C) in Appendix C and integrate using Equation (3C). Long division in Equation (12D) yields

$$F = p_g C r_o \int_0^{2\pi} \frac{d\omega}{a'} - \frac{2d\omega}{a'(2 + a' \cos \omega)} + \frac{b'}{a'} \cos \omega \, d\omega +$$

$$\qquad (13D)$$

$$- \frac{2b' d\omega}{a'^2} + \frac{4b' d\omega}{a'^2(2 + a' \cos \omega)}$$

The third term of the right hand member again integrates to zero, and combining the remaining terms obtains

$$F = p_g C r_o \int_0^{2\pi} \frac{a' - 2b'}{a'^2} \, d\omega + \frac{4b' - 2a'}{a'^2(2 + a' \cos \omega)} \, d\omega \qquad (14D)$$

The first term of this equation is easily integrable, and the second term can be integrated by Equation (3C) of Appendix C. The restriction on Equation (3C) that the integrand remain finite for all real ω is satisfied and

the integrated equation becomes

$$F = p_g C r_0 \left[\frac{a' - 2b'}{a'^2} \, 2\pi + \frac{(4b' - 2a') \, 2\pi}{a'^2 \sqrt{4 - a'^2}} \right] \qquad (15D)$$

Finally after substituting the values for a' and b' from Equation (11D), we obtain for the lateral force on one land of a cocked and displaced piston the equation

$$F_n = \frac{F}{2r_0 C p_g} = \frac{\pi}{(2\tau + 2\gamma \frac{C'}{t} + \gamma \frac{C}{t})^2} \left[\gamma \frac{C}{t} - \frac{2\gamma C}{t \sqrt{4 - (2\tau + 2\gamma \frac{C'}{t} + \gamma \frac{C}{t})^2}} \right]$$

$$(16D)$$

If the piston is of the two land type illustrated in Figure (2b), Equation (16D) is valid for the other land with the difference that τ is the negative of τ for the first land. This dimensionless force is plotted versus $\frac{\gamma}{t} (C + C')$ for the case when $\tau = 0$ in Figure (3).

Inspection of Equation (16D) shows that $\tau > 0$ serves to diminish the lateral force on a land. This is true because the rate of change of the pressure gradient depends upon the rate of change of clearance in the flow region. To develop a large lateral force this gradient must vary rapidly. Therefore, the greatest rate of change of clearance and consequently pressure gradient and lateral force occur when the piston is

only rotated and not displaced. Displacement in any direction, then, serves only to reduce the lateral force.

BIBLIOGRAPHY

1. Bateman, H. *Partial Differential Equations of Mathematical Physics.* New York: Dover, 1944.

2. Blackburn, John F. "Lateral Forces on Hydraulic Pistons." Memorandum: DIC 6387, October 5, 1949.

3. Churchill, Ruel V. *Introduction to Complex Variables and Applications.* New York, Toronto, London: McGraw-Hill, 1948.

4. Goldburg, Arnold. "Elimination of Causes and Effects of Lateral Forces on Hydraulic Pistons." S.M. Thesis, Mechanical Eng. Dept., M.I.T., 1951.

5. Hunsaker, J. C. and Rightmire, B. G. *Engineering Applications of Fluid Mechanics.* New York and London: McGraw-Hill, 1947.

6. Instrumentation Laboratory. "The Pressurized Fluid Bearing for High Precision Instrument Suspension." M.I.T., 1948.

7. Prandtl, L. and Tietjens, O. G. *Applied Hydro- and Aeromechanics.* New York and London: McGraw-Hill, 1934.

8. Prandtl, L. and Tietjens, O. G. *Fundamentals of Hydro- and Aeromechanics.* New York and London: McGraw-Hill, 1934.

9. Timoshenko, S. *Strength of Materials, Part II.* New York: Van Nostrand, 1941, 2nd Ed., pp. 80-83.